Structure of semiconductors in noncrystalline states

Yu. G. Poltavtsev

Usp. Fiz. Nauk **120**, 581–612 (December 1976)

The known results of diffraction investigations of liquid, vitreous, and amorphous (film) semiconductors are examined with an aim at finding the general laws governing the structural changes in the crystal–melt, melt–glass, and crystal (vapor)–amorphous film transitions. These laws are formulated. A classification by structural attributes is proposed for liquid semiconductors. The role of the initial structure of the crystal in the formation of the structure of the short-range order of the melt is considered, the types of singularities of the structural changes accompanying melting in semiconductor–metal and semiconductor–semiconductor transitions are noted.

PACS numbers: 61.20.–p, 61.50.–f, 64.70.Ew, 64.70.Kb

CONTENTS

1. Introduction 969
2. Theoretical Principles of Diffraction Investigations of Noncrystalline Substances 970
3. Results of Investigations of the Structure of the Short-Range Order of Semiconductors in Noncrystalline States 972
4. Principal Features of the General Laws Governing the Structure of Crystalline Semiconductors 981
References 985

1. INTRODUCTION

An unusually large amount of attention is presently being paid to the investigation of semiconductors in noncrystalline states. This is due primarily to the fact that liquids (melts), glasses, and amorphous films are gaining in practical use, predominantly in applications where the use of crystalline substances is impossible or not advantageous. The possibilities of using liquid semiconductors are not yet fully clear, but an exhaustive investigation of their potential use is of great significance for modern electrometallurgy and electrochemistry.

When semiconducting melts are cooled they can solidify without crystallization. In this case glasses are produced, and a special class of them, namely chalcogenide glasses, discovered by N. A. Goryunova and B. T. Kolomiets, has a surprisingly fortunate combination of useful physical properties. The latter, together with the recently discovered phenomenon of switching, causes them to be extensively used in a wide range of fields, including IR optics, quantum electronics, space and computer technology, etc. Chalcogenide glasses offer promise of solving problems in holography and of the development of silver-free photography.

Amorphous semiconductor films are widely used in computer technology and in microelectronics. The method most widely used to produce them is by evaporation on a cold substrate. By varying the technological parameters that influence the molecular composition of the vapors and the character of the interatomic interactions on the substrate, it becomes possible to obtain films with a wide gamut of physical properties.

The practical use of liquids and vitreous semiconductors is based on the fundamental scientific research carried out by Regel',[1–3] who observed the very existence of semiconductivity in the liquid state, and of Kolomiets,[4,5] who found that vitreous semiconductors lend themselves poorly to doping. In 1950, A. F. Ioffe, on the basis of data by A. R. Regel' arrived at conclusions that the periodicity of the crystal (long-range order) turns out to be insignificant for the conversion of electrons into the conduction state, but changes of the short-range order manifest themselves most decisively in the electric properties of semiconductors. As some of the most important first-order problems of the physics of semiconductors, A. F. Ioffe proposed to carry out further investigations of their physical properties, "and also trace the x-ray structure data concerning the short-range order in the solid and liquid states."[6]

Extensive investigations of the temperature-induced variations of the physical properties in the course of melting and in the liquid state, carried out subsequently, have enabled A. R. Regel' to classify all the semiconductors as those melting in via a semiconductor–metal transition and via a semiconductor–semiconductor transition.[7,8] Somewhat later, V. M. Glazov has established[9,10] that the semiconductor–semiconductor transition occurs in the course of melting, and the semiconductor–metal transition extends over a definite temperature interval in the liquid phase. However, not enough attention was paid to the study of the structure of the short-range order of melts by direct diffraction methods. Consequently, until recently the results of predominantly isolated x-ray diffraction investigations of liquid Ge, or III-V semiconductors, and of chalcogenides constituted the totality of our knowledge of this subject. Naturally, there were no solutions to a number of important scientific problems, such as finding the general laws governing the structural changes in different types of semiconductors in the course of melting, on which

the changes of the physical properties are based (particularly, in semiconductor–metal and semiconductor–semiconductor transitions), and assessing the role of the initial structure of the crystal in the evolution of the short-order structure of a melt, the distinguishing features of the interatomic interactions in melts in a wide range of temperatures, etc. Structure investigations of melts have attracted serious attention only recently.

Directly related to structural investigations of melts are investigations of the short-order of glasses. It appears that until recently the only comprehensive theory of glass formation was the kinetic theory of Turnbull and Cohen,[11,12] according to which the condition for vitrification is that the ratios of the free activation energies of the crystallization-center formation and of the crystal growth to the temperature below which crystals can be produced must be large. To apply this theory to concrete materials it is necessary to know the structural features of the melt and of the glass that is formed from it, and also the nature of the atomic structure changes that occur when the melt solidifies.

The study of the formation, of the structure, and of the properties of amorphous films is presently being paid persistent attention. It has been established[13] that there exist two mechanisms of vapor condensation on a substrate, namely vapor–crystal and vapor–liquid. At a critical temperature that depends on the substance, one condensation mechanism gives way to the other, and there exists also an interval of heterogeneous condensation via both mechanisms. In the latter case, as well as in condensation by the vapor–liquid mechanism, amorphous films may be produced. Therefore the amorphous states of matter can be regarded as a possible model of a liquid state in which the main structural elements of the latter are "frozen in." Consequently the study of the structure of the short-range order of amorphous films, as well as of glasses, is best carried out in close connection with investigations of the structure of liquids.

The formulation of the most important primary problems of the physics of semiconductors, given by A. F. Ioffe, and the arguments concerning the advantages of studying the short-range structure of glasses and amorphous films in close connection with the investigation of melts, which were described above, have determined the purpose of this article, namely a critical review of the known results of diffraction investigations of semiconductors in noncrystalline states, with an aim at finding the general laws governing the structural variations in crystal–melt, melt–glass, and crystal–(vapor)–amorphous transitions, on which the changes of the physical properties are based.

2. THEORETICAL PRINCIPLES OF DIFFRACTION INVESTIGATIONS OF NONCRYSTALLINE SUBSTANCES

Diffraction investigations are direct methods of studying the structure of the short-range order of a noncrystalline substance. They are based on the study of the angular distribution of the scattering of coherent radiation, and yield the absolute values of the predominant interatomic distances r_i, coordination numbers Z_i, and the radius R_0 of the ordered arrangement of the atoms. They make it possible to draw conclusions concerning the most probable geometry of the nearest neighbors and the character of the interatomic interactions. The principal equations of diffraction theory[14] are the expressions for the intensity $I_N(\mathbf{s})$ of scattering by an aggregate of N atoms

$$I_N(\mathbf{s}) = f^2(\mathbf{s}) \int p(\mathbf{r}) \exp(-i\mathbf{sr})\, dv_\mathbf{r} \tag{1}$$

and for the structure factor

$$i(\mathbf{s}) = v_1 \int \frac{p(\mathbf{r})}{V} \exp(-i\mathbf{sr})\, dv_\mathbf{r}, \tag{2}$$

in which

$$p(\mathbf{r}) = \int \rho(\mathbf{u})\, \rho(\mathbf{u}+\mathbf{r})\, dv_\mathbf{u} \tag{3}$$

is the generalized Patterson function, $v_1 = V/N$ and $p(\mathbf{r})/V$ are the mean values of the products of the atomic densities $\rho(\mathbf{u})$ at two points, separated by the vector $\mathbf{r}$. All the various expressions for $I_N(\mathbf{s})$ and $i(\mathbf{s})$, which are known in the literature, are only their consequences and correspond to particular assumptions concerning $p(\mathbf{r})$. Let us examine some of them.

A. Case of statistically homogeneous simple inorganic object

The short-range structure of such substances is determined by the statistical function $Z(\mathbf{r})$:

$$Z(\mathbf{r}) = \delta(\mathbf{r}) + \frac{W(\mathbf{r})}{\vartheta_1}, \tag{4}$$

in which the δ function corresponds to the position of the initial atom and $W(\mathbf{r})$ corresponds to the probability of the arrangements of its neighbors, with $W(\mathbf{r}) = 1$ at $|\mathbf{r}| \geq R_0$. The mean value $\langle p(\mathbf{r}) \rangle$ is connected with $Z(\mathbf{r})$ by the relation[15]

$$\left\langle \frac{p(\mathbf{r})}{V} \right\rangle = \frac{Z(\mathbf{r})}{v_1}; \tag{5}$$

For a statistically homogeneous object, formula (2) now goes over into

$$i(\mathbf{s}) = 1 + \frac{1}{v_1}\delta(\mathbf{s}) + \frac{1}{v_1}\int [W(\mathbf{r}) - 1] \exp(-i\mathbf{sr})\, dv_\mathbf{r} \tag{6}$$

and, by using the Fourier transformation, we obtain for the radial atom distribution curve (RADC)

$$4\pi r^2 \rho(r) = 4\pi r^2 \rho_0 + \frac{2r}{\pi}\int \left[i(s) - 1 - \frac{1}{v_1}\delta(s) \right] s \sin sr\, ds. \tag{7}$$

The positions of the maxima of this curve correspond to the preferred distances to the equally-distant neighbors and are the radii of the coordination spheres, while the areas under them

$$Z_i = \int_{r_i-\Delta r}^{r_i+\Delta r} 4\pi r^2 \rho(r)\, dr \tag{8}$$

are the coordination numbers.

B. Case of statistically homogeneous simple organic object

By statistically homogeneous organic objects we mean objects that are identical with respect to structure to the volume cut out by the plotted surface in the unbounded material. If $\sigma(\mathbf{r})$ is the shape factor, then

$$\langle p(\mathbf{r})\rangle = \frac{V}{v_1} Z(\mathbf{r})\, V(\mathbf{r}), \tag{9}$$

where

$$V(\mathbf{r}) = \frac{1}{V}\int \sigma(\mathbf{u})\,\sigma(\mathbf{u}+\mathbf{r})\, dv_{\mathbf{u}} \tag{10}$$

is the volume which is common to the object and the "twin" obtained when the object is displaced by a vector $\mathbf{r}$. From among the many properties of $V(\mathbf{r})$ we note that this is a decreasing function, it becomes equal to zero when $|\mathbf{r}|$ is larger than the maximum dimension of the object in the direction $\mathbf{r}$.

Taking (9) and (10) into account, expression (2) for the case of a statistically homogeneous bounded object is transformed into

$$i(s) = 1 + \frac{1}{v_1}\int V(\mathbf{r}) \exp(-is\mathbf{r})\, dv_{\mathbf{r}} + \frac{1}{v_1}\int V(\mathbf{r})\,[W(\mathbf{r})-1]\exp(-is\mathbf{r})\, dv_{\mathbf{r}}. \tag{11}$$

Equation (11) goes over into (6) when $V(\mathbf{r})$ is replaced by unity. Let us estimate the accuracy of such an approximation, without considering the first integral, which corresponds to small-angle scattering.[15] The relative error due to this substitution cannot exceed $\varepsilon = 1 - V(\mathbf{R}_0)$, inasmuch as $W(\mathbf{R}_0) = 1$ and $V(\mathbf{r})$ is a decreasing function. If $\mathbf{R}$ is the maximum object dimension, then $V(\mathbf{R}_0) = (\mathbf{R} - \mathbf{R}_0)/\mathbf{R}$ and the error is $\varepsilon = \mathbf{R}_0/\mathbf{R}$. The experimental data show that for real objects $R_0 \sim 10$–20 Å and $|\mathbf{R}|$ is a macroscopic quantity. Even if $R = 1$ mm, we still have $\varepsilon \sim 10^{-6}$, i.e., much less than the accuracy of realistic precision measurements of diffraction patterns with modern diffractometers (1–2%).

C. Multicomponent noncrystalline substances. Particular case of binary melts

The short-range order structure of multicomponent noncrystalline substances is described by the partial RADC $\rho_{i,j}(r)$, which are connected with the RADC $U(r)$ by the relation[16]

$$4\pi r^2 U(r) \equiv 4\pi r^2 \sum_{i,j} n_i k_i k_j \rho_{i,j}(r) = 4\pi r^2 \Big(\sum_i n_i k_i\Big)^2 \rho_0 + \frac{2r}{\pi}\int [i(s)-1]\, s \sin sr\, ds, \tag{12}$$

where n_i is the concentration of the i-th component, ρ_0 is the average density, $k_i^2 = \langle f_i^2(s)/\sum n_i f_i^2(s)\rangle$, and $i(s)$ is the common structure factor:

$$i(s) = 1 + \frac{(I_N(s)/N) - \sum_i n_i f_i^2(s)}{\sum_i n_i f_i^2(s)}. \tag{13}$$

The common RADC $U(r)$ is a linear combination of $\rho_{i,j}(r)$. It follows from (12) that owing to the difference between the scattering amplitudes the $U(r)$ will be determined to a considerable degree by the relative placement of the components with larger $f(s)$, rather than by the arrangement of the atoms with smaller scattering amplitudes. Therefore the positions of its maxima do not correspond to the real values of the preferred interatomic distances, but turn out to be shifted towards the values of the distances between atoms with large $f(s)$, and the numerous distances between the atoms with small $f(s)$ are less noticeable. The areas

$$A_i = \int_{r_i-\Delta r}^{r_i+\Delta r} 4\pi r^2 U(r)\, dr \tag{14}$$

under the maxima of the common RADC do not correspond, just as for simple substances, to the values of the coordination numbers. Therefore these RADC are interpreted by testing various models of the short-range order structures and by invoking data obtained from thermodynamic and physico-chemical investigations—naturally, sufficiently reliable results are confined mainly to the information pertaining to the first coordination sphere.

For binary substances, expression (13) for the general structure factor can be written in the form[17]

$$i(s) - 1 = n_1 k_1^2 [i_{11}(s) - 1] + n_2 k_2^2 [i_{22}(s) - 1] + 2n_1 k_1 k_2 [i_{21}(s) - 1], \tag{15}$$

where $i_{i,j}(s)$ are partial structure factors defined by the relation

$$i_{i,j}(s) = 1 + \int 4\pi r [\rho_{i,j}(r) - n_i \rho_0] \frac{\sin sr}{s}\, dr. \tag{16}$$

If the $i_{ij}(s)$ are known, then we can obtain the partial RADC:

$$4\pi r^2 \rho_{i,j}(r) = 4\pi r^2 n_i \rho_0 + \frac{2r}{\pi}\int [i_{i,j}(s) - 1]\, s \sin sr\, ds \tag{17}$$

and the partial coordination numbers

$$Z_{i,j} = \int 4\pi r^2 \rho_{i,j}(r)\, dr, \tag{18}$$

which are connected with the areas under the maxima of the common RADC by the relation

$$A = n_1 k_1^2 Z_{11} + n_2 k_2^2 Z_{22} + 2n_1 k_1 k_2 Z_{21}. \tag{19}$$

For a complete description of the structure of the short-range order of binary noncrystalline substances it is necessary to know three partial RADC, which are determined by taking the Fourier transforms of the three corresponding structure factors. In an individual diffraction experiment, however, one measures only a common structure factor, which is a linear combination of $i_{i,j}(s)$. The weighting factors in (15) depend on the concentration and on the atomic amplitudes of the scattering, and the latter are different for different types of radiation. Therefore if we measure $i(s)$ in three experiments—x-ray diffraction, neutron diffraction, and electron diffraction—then, in principle, we can find the partial structure factors (and from them also the partial RADC), as solutions of a system of three equations,

each of which is in the form (15). No such experiment has been performed as yet, but there is a known combination of x-ray diffraction and neutron-diffraction data for a special case.[18] In[19] use is made of the fact that the atomic amplitudes for a neutron scattering are different for the different isotopes. Therefore, by carrying out three neutron-diffraction experiments with samples of the same composition but containing different isotopes of one of the components it is also possible to find in similar fashion the partial structure factors.

Particular interest attaches to the case of binary melts. The experimental data show that the distinctive character of the thermal motion of the atoms in these melts can lead either to elimination of the difference between the force fields of the components, or to a preferred existence of groups of atoms with energywise most favored short-range order. The first corresponds to a statistical distribution of atoms of different sorts, and the second manifests itself in a similarity of the general structure factors of melts with different concentrations[20] and in their proximity to the superposition of general structure factors of "reference" compositions.[21] In this case there are grounds for assuming that the partial structure factors do not depend on the component concentration[21,22] and, remaining within the framework of one diffraction method, say x-ray diffraction, we can determine experimentally $i_{i,j}(s)$ and $4\pi r^2\rho_{i,j}(r)$, by measuring the general structure factors $i'(s)$ of a number of alloys of different compositions, as solutions of systems of equations of the type

$$\left.\begin{aligned} i'(s)-1 &= n_1'k_1'^2[i_{11}(s)-1]+n_2'k_2'^2[i_{22}(s)]-1]+2n_1'k_1'k_2'[i_{21}(s)-1],\\ i''(s)-1 &= n_1''k_1''^2[i_{11}(s)-1]+n_2''k_2''^2[i_{22}(s)-1]+2n_1''k_1''k_2''[i_{21}(s)-1],\\ &\cdots\cdots\cdots\cdots\cdots\cdots\cdots\cdots\cdots\cdots\cdots\cdots\end{aligned}\right\} \quad (20)$$

The partial structure factors obtained from (20) correspond, naturally, to the $i_{i,j}(s)$ for a melt having a concrete composition, at an accuracy that depends on the assumption made. The accuracy of the approximation corresponds to the accuracy with which Eq. (19) is satisfied.[23] The structure factors of alloys of the systems Ag–Sn[21], Au–Sn[24], Cu–Sn[25], Ag–Mg[26], Mg–Sn[23] were determined in this manner. It turned out that the $i_{i,j}(s)$ are very sensitive to the errors in the measurements of $i'(s)$,[21] so that it becomes necessary to investigate melts with more than three compositions and to obtain the partial structure factors by solving the overdefined systems (20). At a given experimental error, the accuracy of the calculations[1)] of $i_{i,j}(s)$ increases with increasing number of equations in the systems, i.e., when values of $i'(s)$ of as large a number of samples of various compositions as possible are used. If the character of the interatomic interactions in the melts is not strongly altered when the temperature is varied, then it is possible to calculate $i_{i,j}(s)$ by using the measured values of $i'(s)$ at different temperatures. The number of equations in the system (20) is increased in this case when $i'(s)$ is used for only three alloys, but the obtained $i_{i,j}(s)$ are now averaged over the concentration and temperature intervals.[17]

[1)] *By the method of least squares.*

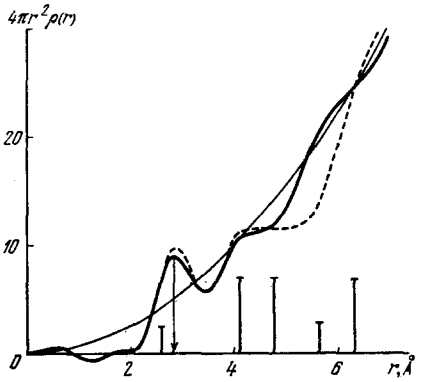

FIG. 1. Plot of radial distribution of the atoms in liquid Si.

3. RESULTS OF INVESTIGATIONS OF THE STRUCTURE OF THE SHORT-RANGE ORDER OF SEMICONDUCTORS IN NONCRYSTALLINE STATES

A. Liquid semiconductors (melts)

1) *Elemental semiconductors.* Among the elemental semiconductors are those of group IV and chalcogenides. Hendus[27] was the first to investigate the structure of molten Ge (T_m = 937 °C) at 1000 °C. On the right-hand branch of the intensity curve of the scattered x rays he noted a sideband maximum previously observed on the intensity curves of liquid semimetals and attributed to the "loose" packing of the atoms.[28] The radius of the first coordinate sphere and the coordination number were found to be r_1 = 2.7 Å and Z_1 = 8. Comparison of these data with the corresponding values for the crystal r_{1k} = 2.44 Å and Z_{1k} = 4 has shown that the melting is accompanied by a substantial change in the short-range order, and consequently also in the character of the interatomic bonds. This explained why the germanium loses its semiconducting properties following the crystal–melt transition. Subsequent investigations of the melt at high (1000–1300 °C) temperature[29–32] yield results that work in sufficiently good agreement with one another: r_1 = 2.73–2.83 Å, Z_1 = 5.8–7.1; it was established that the structure of the short-range order of liquid Ge is well described by the model of "smeared" primitive cubic (PC) lattice. When the melt temperature is lowered to 940[33] and 985[30] °C, the coordination number has a tendency to decrease, but r_1 remains practically unchanged. The octahedral coordination of the nearest neighbors is distorted and the structure of the short-range order of the melt acquires features that are similar to the structure of β-tin.[30,31]

Liquid Si (T_m = 1414 °C) was first investigated in[34] and the values r_1 = 2.8 Å and Z_1 = 6.7 were obtained at 1500 °C. Figure 1 shows the RADC in the melt. The dashed curve, which was calculated in accordance with[35,36], represents the RADC in the crystal at $T = T_m$. These curves describe entirely different atom distributions, thus attesting to breaking of the covalent bonds of the crystal on going to the molten state. The short-range structure of the molten Si, just as that of the Ge, agrees well with the model of the "smeared" PS lattice—

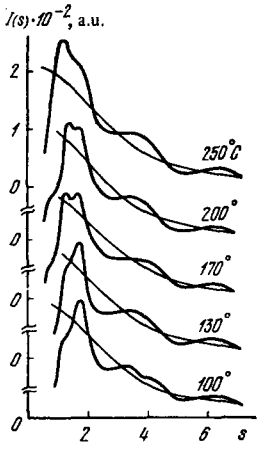

FIG. 2. Intensity plots of x rays scattered by liquid S.

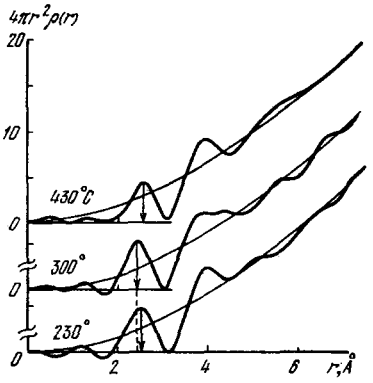

FIG. 4. Radial distribution of the atoms in liquid Se.

this is not surprising, since Ge and Si are crystal-chemical analogs. On this basis, one would expect the octahedral coordination of the neighbors to become distorted with decreasing melt temperature, but an investigation[37] of liquid Si at 1420, 1520, and 1650 °C shows no such distortion.

The valence configuration of the chalcogenide atoms ns^2np^4 presupposes two covalent bonds with nearest neighbors, which can be either in the *cis* or in the *trans* positions.[38] The former corresponds to formation of ring molecules, and the latter to long atomic chains. With increasing atomic number of the element, the tendency to the realization of the *cis* positions of the neighbors decreases.

Meyer[39] described more than thirty allotropic modifications of sulfur, noting that only four of them are stable: rhombic (α-form), monoclinic (β-form), molecules (S_α) in the form of eight-member rings, and biradical chains (S_μ). Many metastable modifications can be obtained from the liquid state, and the highly critical parameters are the initial temperature of the melt and the rate of its cooling.

The structure of liquid sulfur ($T_m = 112$ °C) was investigated many times[40–42]; the most interesting of the earlier papers seems to us to be that of Gingrich,[43] who investigated the melt in the interval 124–340 °C. It was found that heating the melt leads to a shift of the first two maxima of the critical intensity of the scattered x rays towards smaller s. The RADC in liquid sulfur turned out to be similar for all temperatures, while $r_1 = 2.07$ Å and $Z_1 = 1.7$ remained unchanged. Later on Prins[44] and Thompson and Gingrich[45] have shown that when liquid sulfur is heated to 340 °C the position of the first maximum of the intensity curve remains unchanged, but an additional maximum appears on its left slope, with an intensity that depends strongly on the temperature. This was regarded as the temperature-induced change in the position of the first maximum, since the photography geometry in[43] did not permit resolution of the additional maximum. In[45], the value of r_1 was found to be 2.07 Å, while Z_1 turned out to decrease monotonically from 2.22 (at 120 °C) to 1.97 (at 300 °C).

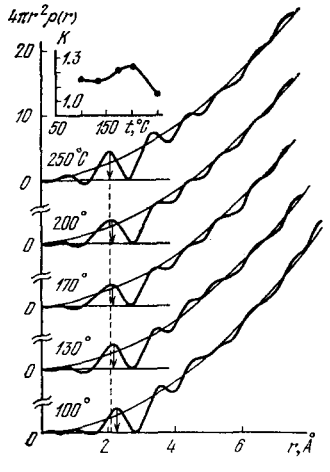

FIG. 3. Radial distribution of the atoms in liquid S. The temperature dependence of the asymmetry K of the first maximum is shown.

Precision measurements of the intensity curves of x rays scattered by liquid sulfur were recently carried out[46] at 100–250 °C. These curves, which are shown in Fig. 2, can be divided into three groups in accordance with the temperature intervals 100–130 °C, 170–200 °C, and 250 °C. The differences between the intensity curves offers undisputed evidence that the structure of the short-range of the alloy is different.

Figure 3 shows RADC in liquid sulfur in accordance with[48], from which the values $r_1 = 2.20$ Å, and $Z_1 = 2.4$ for 100 °C, $r_1 = 2.15$ Å and $Z_1 = 2.4$ for 170 °C and $r_1 = 2.08$ Å, $Z_1 = 2.6$ for 250 °C were determined. Raising the melt temperature leads not only to a decrease of r_1, but also to a change of the asymmetry K of the first RADC maximum on the side of small r, with the maximum values of K corresponding to temperatures 170–200 °C. This is attributed[46] to the presence of low-molecular formations of S_2 and S_3 in the alloy besides the "molecules" S_λ; the latter are the predominant structural elements of the melt only at 100–130 °C.

Selenium ($T_m = 220$ °C) crystallizes in two monoclinic modifications (α and β) and one hexagonal modification[47]; only the latter is thermodynamically stable. The monoclinic modifications are made up of Se_8 "molecules," the shortest distance in which is $r'_{1k} = 2.34$ Å, and the hexagonal modification is made up of helical atomic chains with $r''_{1k} = 2.37$ Å. The structure of liquid Se was investigated in[48–52], and the results were in good agreement with one another. Figure 4 shows the

RADC in the melt at 230, 300, and 430 °C, taken from[52]; the position of the first RADC maximum in the melt at 230 °C, namely $r_1 = 2.38$ Å, is close to r''_{1k}, at 300 °C we have $r_1 \approx r'_{1k}$, and at 430 °C the shortest interatomic distance again turns out to be close to r''_{1k}. This suggests that the predominant structural elements of the melt are helical chains, just as in the hexagonal modification of the crystal, but there exists a temperature interval near 300 °C where the existence of Se_8 "molecules" is energywise also favored. Richter[48] admits of the possible existence in the melt, of flat chains and Se_6 "molecules" besides the atomic chains and the Se_8 "molecules."

Tellurium ($T_m = 442$ °C) crystallizes into a hexagonal lattice constructed of zigzag-shaped atomic chains with $r_{1k} = 2.835$ Å and $Z_{1k} = 2$.[47] The first investigation of liquid Te at 485 and 610 °C was made by Buschert[53]; the coordination number for low temperatures was found to be $Z_1 = 2.3$, and the first RADC maximum was located at $r_1 = 2.9$ Å. Since $r_1 > r_{1k}$ and $Z_1 \approx Z_{1k}$, it was concluded that when the crystal melts the chain character of the structure is preserved, but the interatomic distances in the chains increase somewhat.

The short-range order of molten tellurium near T_m was investigated also in[54], the values $r_1 = 2.95$ Å and $Z_1 = 2.4$ for the temperatures 450 and 510 °C turned out to be close to the data of[53]. Two approaches to the interpretation of the RADC were made, with r_{1k} assumed to increase in the first and to remain constant in the second. In the latter case it can be concluded that the structural elements of the melt at 450 °C are atomic chains with $r_1 = r_{1k}$, which calculations have shown to contain $N = 20$ atoms, and heating to 510 °C decreases N to 10.

Models of the short-range structure of molten Te near T_m, which follow from both approaches to the interpretation of the RADC, are close. The structure elements of the melt in these models are atomic chains that differ only in the value of r_1. According to the known diffraction data, no preference can be given to either. Raising the temperature of the liquid tellurium to 1700 °C increases the coordination number to ~ 6 and increases r_1 to 3.07 Å.[55]

2) *Semiconductors of the* III-V *type.* Semiconducting III-V compounds crystallize in a ZnS lattice, in which

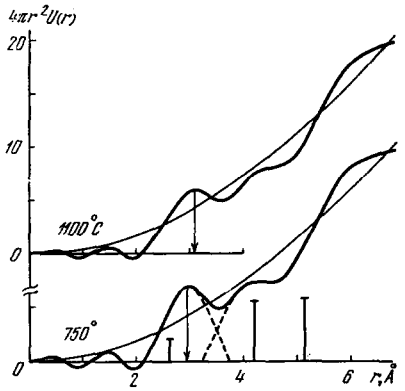

FIG. 5. Plots of the radial distribution of the atoms in liquid GaSb.

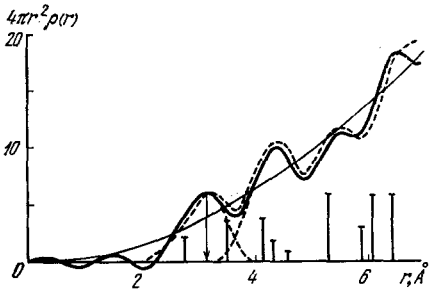

FIG. 6. Plots of radial distribution of the atoms in liquid InTe. Dashed—RADC in "smeared" PC lattice.

the "loose" packing of the atoms is due predominantly to the covalent character of the interatomic bonds.[56] Investigations in the liquid phase were made on GaSb,[57] InSb,[58,59] and InAs.[60]

An x-ray diffraction investigation of GaSb ($T_m = 712$ °C) was carried out at 750 and 1100 °C. Figure 5 shows the RADC in the melt, with the vertical segments indicating the positions of the coordination spheres in the crystal: $r_{1k} = 2.64$ Å, $r_{2k} = 4.30$ Å, $r_{3k} = 5.07$ Å, $Z_{1k\,Ga}(Sb) = Z_{1k\,Sb}(Ga) = 4$, $Z_{2k\,Ga}(Ga) = Z_{2k\,Sb}(Sb) = 12$. For the temperature 750 °C the results obtained were $r_1 = 3.0$ Å, $Z_{1\,Ga}(Sb) = Z_{1\,Sb}(Ga) = 5.8$, $r_2/r_1 = \sqrt{2}$ and it was concluded that the structure of the melt agrees well with the model of the "smeared" PC lattice. An increase of r_{1k} and Z_{1k} in the crystal–melt transition is undoubtedly due to the breaking of the covalent interatomic bonds and explains the ensuing loss of the semiconducting properties.[61]

Heating the melt to 1100 °C causes a transition to a statistical distribution of atoms of different sorts and to slight increases of r_1 and Z_1. Investigations of the short-range structure of liquid indium antimonide and arsenide yielded similar results.

3) *Semiconducting compounds of the* III-VI *system.* The elements of the IIIB subgroup of the periodic system enter into a large number of compounds with chalcogenides, the most typical among which are $A^{III}B^{VI}$, $A_2^{III}B_2^{VI}$, and Tl_2B^{VI}; the remaining compounds are unstable. From among the compounds of equiatomic composition in the liquid state, investigations were made of indium monotelluride InTe ($T_m = 696$ °C), which crystallizes into a tetragonal lattice. In the latter, the atoms of different sorts are arranged in layers, and there are indium atoms of two sorts. The atoms In_{II} are surrounded in a tetragonal prism by eight Te atoms at distances $r''_{1k} = 3.57$ Å, while the atoms In_I are coordinate tetrahedrally at a smaller distance $r_{1k} = 2.78$ Å. The bond of In_{II} with the nearest neighbors is effected by p-electrons, and the valence electrons of In_I are in the sp^3-hybridization state.

Figure 6 shows the RADC in liquid InTe at 750 °C[62]; the position of its first maximum $r_1 = 3.24$ Å is close to the average of r'_{1k} and r''_{1k}, with $Z_1 = 6.2$ and $Z_2 = 9.5$. A good model of the short-range structure of the melt is the "smeared" PC lattice with parameter $a = r_1$.

The compounds $A_2^{III}B_3^{IV}$ crystallize in the ZnS structure types that contain defects with respect to the metal atoms occupying 1/3 of all the tetrahedral voids of the

fcc lattice made up by the chalcogenide atoms. Each B^{III} atom is thus surrounded on three sides by A^{III} atoms and has a vacancy on the fourth side. It is assumed[63] that the electron clouds of two unpaired electrons of the B^{VI} atoms are redistributed in such a way that a pair of electrons belonging to the anion will belong simultaneously to two atoms, thereby effecting the bond. On the vacancy side there are now four filled two-electron clouds from each of the four B^{VI} atoms surrounding the defects. If it is assumed that these clouds can be formally ascribed also to the same defect, then the vacancy turns out to be connected with each B^{VI} atom by a two-electron "bridge," just as an ordinary anion.

The structure of the short-range order of the $A_2^{III}B_3^{VI}$ compounds was investigated with In_2Te_3 ($T_m = 667\,^\circ C$) as an example. Figure 7 shows the RADC in the melt at a temperature 700 °C,[64] the results being $r_1 = 2.90$ Å, $Z_{1\,Te}(In) = 3.75$, and $Z_{1\,In}(Te) = 2.50$, whereas in the high-temperature β-form of the crystal we have $r_{1k} = 2.67$ Å, $Z_{1k\,Te}(In) = 4$, $Z_{1k\,In}(Te) = 2.66$. Melting of indium telluride thus leads to a small decrease of the coordination numbers and to an increase of the radius of the first coordination sphere, i.e., to a looser packing of the atoms, which is typical of the crystal. It is interesting that InTe and In_2Te_3, which differ by only 10 at.% Te in composition, have essentially different short-range structures in the molten state.

Thallium selenide has in the crystalline state a tetragonal lattice, in which the atoms are arranged in layers or form Tl_2Se "molecules." The principal interaction is between the layers, is stronger than the ion interaction, and has a covalent component. The bond between the atoms of the layers and the Tl_2Se "molecules" is of the same type.

Figure 8 shows RADC in molten Tl_2Se ($T_m = 390\,^\circ C$) at 460 °C and the RADC calculated from the Debye pattern of the polycrystalline sample at 20 °C. The presented radial curves exhibit substantial similarities and certain differences. Among the latter, in particular, is the presence of a maximum on the RADC at $r' = 2.4$ Å. It appears that this maximum is not a false one, for as the melt temperature rises, when the integral width of the structural maxima is increased (and when the upper limit of integration in the calculation of the RADC is raised), this maximum does not vanish and does not shift.[64]

The similarity of the RADC in the molten and crystalline Tl_2Se offers undisputed evidence that the packing of the atoms is not altered significantly by the melting. Then the presence of a maximum at r' can be regarded

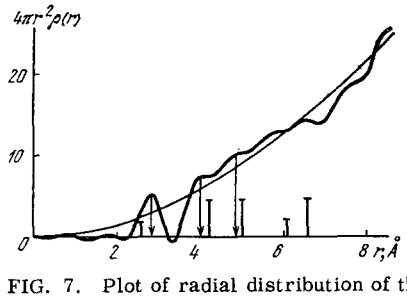

FIG. 7. Plot of radial distribution of the atoms in liquid In_2Te_3.

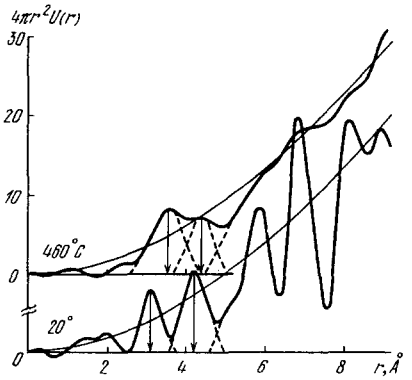

FIG. 8. Plots of radial distribution of the atoms in crystalline (20 °C) and liquid (460 °C) Tl_2Se.

as evidence that the melt is polygenous, namely "crystal-like" groupings of atoms coexist with groupings in which the valence of the Tl atoms differs from +1.

4) *Semiconductors of* IV-VI *type.* In accordance with the type of the crystal structure, IV-VI semiconductors are divided into two groups.[65] The first includes selenides and sulfides of Ge and Sn, as well as the low-temperature modification GeTe (I), all of which have an orthorhombic structure. This structure can be regarded as the structure of black phosphorus, made up of atomic chains packed in such a way that each atom has a distorted octahedral coordination of neighbors. The second group includes chalcogenides of Pb, Sn telleride, and the high-temperature modification GeTe (II), in which the packing of the atomic chains results in a crystal lattice of the NaCl type.

The short-range structure of IV-VI semiconductors of both groups was investigated with GeSe and GeTe as examples. Figure 9 shows RADC in the melts near T_m, the positions of the first maxima of these curves r_1 are smaller than the shortest interatomic distances in the corresponding crystals. The coordination numbers in liquid GeSe were found to be $Z_1 = 4$ and $Z_2 \approx 10$, thus indicating a predominant tetrahedral coordination of the nearest neighbors. These data are interpreted as evidence of enhancement of the covalent component of the interatomic bonds and an appreciable change in the packing of the atoms when the crystal is molten, respectively. The structural changes of GeTe in the crystal–melt

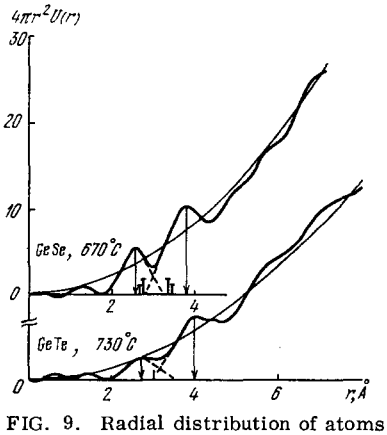

FIG. 9. Radial distribution of atoms in liquid GeSe and GeTe.

transition are similar, but in this case one can assume also the existence of "crystal-like" groups of atoms in the melt.

5) *Melts of the arsenic–sulfur system.* In the As–S system there exist the compounds As_2S_2, As_2S_3, and As_2S_5; the last one is unstable. Arsenic trisulfide in the crystalline state has a monoclinic lattice, in which the atoms are arranged in layers. In the layers we can separate atomic chains joined into 12-link corrugated rings, so that $Z_{1k\,S}(As)=3$, $Z_{1k\,As}(S)=2$, and the distances between the nearest neighbors differ somewhat $r_{1k}=2.15$–2.34 Å. The structure of the As_2S_5 crystal could not be determined, and larger contents of sulfur correspond to the eutectic composition.[67]

The short-range order structure of melts of As_2S_3, $As_{15}S_{85}$, and As_7S_{93} was investigated in[68] in a wide range of temperatures. Figure 10 shows the RADC in these melts, for As_2S_3 at 420 °C the values obtained were $r_1=2.30$ Å, $Z_{1S}(As)=3.8$ $Z_{1\,As}(S)=2.5$. The value of r_1 in the melt falls in the interval of distances between the nearest neighbors in the crystal, but $Z_{1S}(As)$ and $A_{1\,As}(S)$ exceed the corresponding values of $Z_{1\,KS}(As)$ and $Z_{1\,KAs}(S)$. This is interpreted as evidence of a change in the manner in which the atomic chains are joined upon melting. On the basis of the absolute values of the coordination numbers, it was found that the most probable are chains joined into 8-link rings with formation of atomic bands separated by voids.

An increase in the sulfur content leads to a "quasi-eutectic" structure of the melt, the elements of which are groupings of the atoms As_2S_3 and S, the latter being arranged predominantly in the voids between the atomic bands. The RADC calculated for this model in the melt As_7S_{93} is close to the experimental one (see the dashed curve in Fig. 10).

Figure 11 shows the partial difference RADC in As–S melts, calculated from x-ray diffraction experiments.[69] The first two maxima of the $4\pi r^2 g_{S,S}(r)$ curve are located at $r_1=2.1$ Å, $r_2=3.5$ Å, and practically coincide with the corresponding values for liquid sulfur at 100–200 °C. This undoubtedly attests to the existence in the melt of groups of sulfur atoms with the inherent short-range structure of the sulfur. If the melts contain also groupings of As atoms, then the first maximum on the $4\pi r^2 g_{As,As}(r)$ curve should be expected at $r_1=2.42$ Å, which is double the covalent radius of the arsenic atom. However, the first maximum of this curve is located at $r=3.5$ Å, thus indicating that there are no valence bonds between the neighboring As atoms, and consequently there are no such groupings of atoms in the melt. The As atoms are bonded via the sulfur atoms. At an average As–S bond length $r_1=2.43$ Å, the calculated value of the angle between the covalent bonds of the arsenic atoms is S–$\hat{\text{A}}$s–S = 91°. We note that S–$\hat{\text{A}}$s–S = 99° in the crystal.[47]

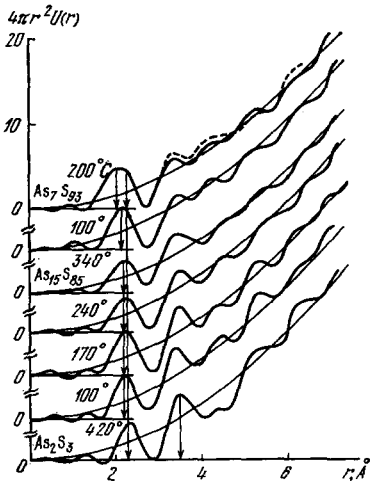

FIG. 10. Plots of the radial distribution of the atoms in the As-S melts.

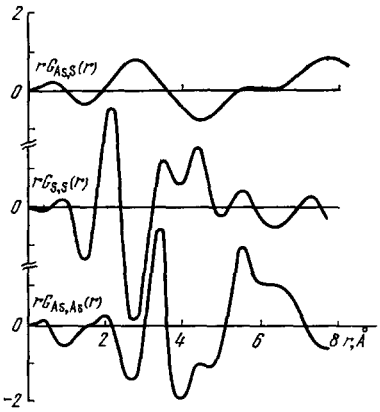

FIG. 11. Partial difference curves of the radial distribution of the atoms in the As–S melts.

The partial RADC $4\pi r^2 g_{As,S}(r)$ is strongly smeared out—this corresponds to the "quasi-eutectic" model described above, since it reflects the differences between the distances between the As atoms located in the atomic bands, and the sulfur atoms located in the bands and in the cavities between them.

6) *Semiconductors of the type* $Sb_2B_3^{VI}$. Compounds of antimony with chalcogens can be subdivided in accordance with the crystal structure[65] into two groups with the structure of tetradymite and Sb_2S_3.

Antimony telluride Sb_2Te_3 ($T_m=622$ °C) has a tetradymite lattice, the unit cell of which is a superposition of three five-layer stacks consisting of layers of atoms, the latter containing only atoms of one sort. The atoms of the layers in the stacks are arranged in the sequence ... Te^1–Sb–Te^2–Sb–Te^1..., and the approximately realized coordination of the nearest neighbors is octahedral with $r_{1Sb-Te^1}=3.06$ Å, $r_{1Sb-Te^2}=3.16$ Å, and $r_{1Te^1\ldots Te^1}=3.62$ Å. When antimony telluride is melted, the weak $Te^1\ldots Te^1$ bonds between the neighboring stacks are partially destroyed, and heating the melt leads to their complete destruction[70]—the calculated mean values of the interatomic distance $r_{1p}=3.11$ Å and of the coordination number $Z_{1p}=4.8$ are practically equal to the corresponding values for the melt at 680 °C.

Antimony selenide Sb_2Se_3 has a crystal lattice of the Sb_2S_3 type, which is made up of corrugated atomic chains joined into ribbons.[65] Van der Waals forces act between the ribbons, and covalent forces, which are subdivided into "strong" and "weak," corresponding to the differences between the shortest interatomic distances, act inside the atomic chains. When the crystal melts,

the bonds between the ribbons are destroyed and apparently also the "weak" bonds between the atoms in the chains. This leads to significant changes in the packing of the atoms.[70]

7) *Semiconductors of the type* $A^{V}B_3^{VII}$. The tri-iodides of As, Sb, and Bi are isomorphic and crystallize in a form analogous to the structure of lead iodide, where each third position of the metal atoms is vacant. The atoms of I form double layers, between which are located the atoms of A^{V}. The structure elements of the crystals are the pyramids $A^{V}I_{6/2}$, with common vertices joined, so that $Z_{1I}(A^{V}) = 6$ and $Z_{1A^{V}}(I) = 2$. To explain why the coordination numbers of the atoms in the crystal exceed their valences, Krebs[75] represented the interatomic A^{V}–B^{VII} bonds in the form of superpositions of series of valence structures that differ in their covalent and donor-acceptor bonds. When antimony and arsenic tri-iodide are melted, the double layers made up of the iodine atoms are destroyed, and the structure elements of the melt become the "molecules" AsI_3, SbI_3 with $Z_{1I}(As, Sb) = 3$ and $Z_{1\,As,Sb}(I) = 1$, which apparently have the form of trigonal pyramids, the bases of which are made up of three atoms that are covalently bound with the As(Sb) atoms situated at the fourth vertex. To explain the character of the interatomic bonds in the melt it is not necessary to assume complicated valence structures, as for a crystal: it suffices to assume that only the p electrons with unpaired spins from the atoms A^{V} and B^{VII} take part in the bond.

B. Vitreous semiconductors

1) *Chalcogens.* By cooling the melt, it is easy to obtain S and Se in the form of glasses. Thompson and Gingrich[45] obtained the RADC for vitreous (so called plastic) sulfur. Just as for the melt, the values obtained for it were $r_1 = 2.07$ Å and $Z_1 \simeq 2$. When vitreous sulfur becomes contaminated with atmospheric nitrogen, it crystallizes,[72] and the presence of sharp diffraction peaks on the intensity curve was observed by us 2–3 hours after the start of aging at room temperature.

The short-range order structure of the vitreous selenium was investigated numerous times[52,73–76]; Hendus[77] was apparently the first to calculate the RADC and to compare the data with the structure of the hexagonal crystal. In[73], vitreous samples were obtained by quenching the melt in water from a temperature 525 °C. To compare the short-range order structure of Se in the vitreous and crystalline states, the RADC in the glass were compared with the radial curves calculated for polycrystalline samples. It was assumed that the packing of the structure units in each crystal was identical, and that their dimensions and the dispersions of the coordination spheres were parameters subject to adjustment. A comparison of the experimental RADC with that calculated for the hexagonal modification of the crystal has shown that their difference begins already with the left-hand branch of the second maximum. This can be regarded as evidence of a less closer packing of the atomic chains in the vitreous sample. We therefore calculated also the RADC in hexagonal Se with increasing distance between the neighboring chains while conserving the arrangements of the atoms in chains themselves. In this case it became possible to obtain agreement between both radial curves in a distance interval that included the first and second maxima, but their discrepancy over large distances is large. Similar calculations were performed for polycrystals of α and β monoclinic modifications. In this case it is possible to obtain better agreement between the calculated and experimental RADC, but the differences at large distances remain significant. This has shown that none of the "crystalline" models corresponds to the structure of the short-range order of glass-like selenium.

In[52], a study was made of the structure correspondence between the melt and the glass. The RADC in molten Se was compared with the radial curve in the vitreous sample. The partial similarity of the structure of the short-range order of the glass and of the melt, limited by the proximity of the values of r_1 and z_1, was noted.

2) *Alloys of the arsenic–sulfur and arsenic–selenium systems.* The limits of the region of vitrification in the As–S system were established in[78]; it was found that stable glasses are obtained at concentrations 15–46 at.% As, while glasses rich in sulfur crystallize in the course of time. Vaĭpolin and Porai-Koshitz[79,80] were the first to investigate the short-range structure of vitreous chalcogenides of arsenic; a glass with composition As_2S_3 was subsequently investigated in[81,82]. According to the data of these papers in vitreous As_2S_3 we have As_2S_3 $r_1 = 2.25$–2.30 Å, $Z_{1S}(As) \simeq 3$. $Z_{1\,As}(S) \simeq 2$, just as in the crystal, but the RADC cited in these papers differ greatly, starting with the region of the second maximum. This indicates that the samples investigated by the different authors were not identical.

The close values of the coordination numbers in vitreous As_2S_3 are regarded by Vaĭpolin and by Porai-Koshitz as evidence of a layered arrangement of the atoms. An analysis of the RADC has shown that the glass can consist of chains, layers, and atomic bands of any width. In[83,84], an investigation was made of the structure of the short-range order of As–S glasses of various compositions. The authors assume that in the As_2S_3 glasses the atomic layers consist not only of 12-member rings, as in the crystal, but also of 8-, 10-, and 14-member rings, which can be produced when the method of joining the atomic chains is altered. It was found that an increase in the sulfur content leads to formation of –S–S– chains together with groupings that contain atoms of different sorts; at a sulfur concentration higher than ~ 80 at.%, formation of new structural units of "molecules" $S_\lambda \equiv S_8$ becomes possible.

The influence of γ rays on the structure of the short-range order of vitreous As_2S_3 was investigated in[85]. Figure 12 shows the RADC in the initial and in irradiated samples, and the irradiation dose is indicated. The values of the coordination numbers $Z_{1S}(As) = 4.2$ and $Z_{1\,As}(S) = 2.8$ obtained for the glass decreased in this case to their values in the crystal, the asymmetry of the second maximum of the RADC increased, and a new maximum appeared at $r = 4.6$ Å, corresponding approximately to the distance between the layers in the crystal. IR spectroscopy investigations[86] have shown that in the As_2S_3

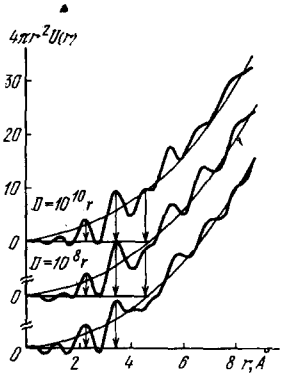

FIG. 12. Radial distribution curves of the atoms in the initial and γ-bombarded samples of vitreous As_2S_3 (the doses are indicated).

glass there exist different shortest distances between the nearest neighbors, just as in a crystal, but the manners of packing of the structure elements in these states are different.

X-ray diffraction investigations of glasses of the As–Se system were carried out in[79,80,87,88]. Vaĭpolin and Porai-Koshitz[79,80] calculated the RADC in vitreous As_2Se_3 and obtained $r_1 = 2.44$ Å, $Z_{1\,Se}(As) = 3.5$, and $Z_{1\,As}(Se) = 2.4$. The authors describe its short-range structure, which consists of atomic layers just as in the structure of the crystal, but more corrugated. Their mutual placements are assumed to be such that there are sites at which the As atoms are coordinated octahedrally. Consequently, the values of the coordination numbers for the glass exceed the corresponding values $Z_{1k\,Se}(As) = 3$ and $Z_{1k\,As}(Se) = 2$ for the crystal.

As–Se glasses containing 3–50 at.% As were investigated in[87]. The area under the first maximum of the RADC in the samples was close to that calculated for a model assuming a coordination 3 for the arsenic atoms and a coordination 2 for the selenium atoms. The position of the first RADC maximum varies linearly with composition for 6–36 at.% As. This corresponds to Vegard's law for solutions, but is valid also for the model of the microinhomogeneous structure ("quasi-eutectic"), in which the elements are Se and As_2Se_3 regions. The available data do not make it possible to give preference to either of these models. No definite laws were revealed in the variations of the positions of the second maximum of the RADC.

It is of interest to compare the RADC in glasses and crystals of compositon AsSe or As_2Se_3. It was found that the positions of the first and second maxima of these curves coincide, but the area under the second maximum of the RADC is smaller in both glasses than in the corresponding crystals, i.e., the structural difference between the crystal and the glass manifests itself already in the second or third coordination sphere. The structural correspondence between the glass and the melt for As_2Se_3 and AsSe was investigated by us in[89]. We have found that for As_2Se_3 the similarity of the short-range structure extends over an interval of distances including the first and second maxima of the RADC, and the AsSe compound is unstable and the structural similarity for it in the vitreous and molten states is less clearly pronounced.

3) *Germanium chalcogenides.* In the systems Ge–S and G–Se there exist compounds GeS(Se) and $GeS_2(Se_2)$, with the monochalcogenides having an orthorhombic structure and the dichalcogenides having a lattice of the CdI_2 type.[90]

Two regions of vitrification in the Ge–S system are reported in[91], corresponding to the intervals 0–33 at.% Ge and 40–43 at.% Ge. Rouland *et al.*[92] investigated the structure of the short-range order of the glasses $Ge_{33}S_{67}$ and $Ge_{42}S_{58}$. The positions of the RADC maxima in the glass $Ge_{33}S_{67}$ were close to the average distances in the GeS_2 crystal: on this basis, the authors have concluded that the character of the interatomic bonds is similar. For the model of a disordered grid with $Z_{1S}(Ge) = 4$ and $Z_{1Ge}(S) = 2$, the calculated value of the area under the first maximum of the RADC is close to the experimental one.

The position of the first maximum $r_1 = 2.3$ Å of the RADC in the $Ge_{42}S_{58}$ glass is much smaller than the average distance $r_{1k} = 2.76$ Å to the nearest neighbors in the GeS crystal. This is regarded as evidence of enhancement of the covalent component of the interatomic bond on going from the crystal to the glass. It was impossible to obtain an unambiguous model of the short-range order structure for glass of this composition.

Using a glass with composition Ge_2S_3 as an example, we have investigated the structural correspondence between the glass and the melt. It was found that raising the temperature of the vitreous sample to 400 °C leads to a strong smearing of the maxima of the RADC, but the areas under them remain unchanged.

In[93,94] a study was made of the short-range structure of glasses of the Ge–Se system. For samples close in composition to $GeSe_2$, the values obtained were $Z_{1\,Se}(Ge) = 4$ and $Z_{1\,Ge}(Se) = 2$, i.e., the short-range orders in the glass and the crystal are similar. We note that this similarity is limited to the first coordination sphere, and that at larger distances the RADC are different in the crystal and in the glass.

A glass with composition Ge_9Se_{91} has a microheterogeneous structure, the elements of which are the groupings of the atoms $GeSe_2$ and Se.

4) *Alloys of the systems* A^{IV}–B^{V}–C^{VI}. An x-ray diffraction study of the glasses $Ge_{20}As_{40}Se_{40}$, $Ge_{35}As_{40}Se_{25}$ and $Ge_{45}As_{30}Se_{25}$ was carried out in[93]. It was established that the position of the first maximum of the RADC changes little with changing composition and corresponds to the sum of the covalent radii of the atoms of the components. The calculated values of the areas under the first maximum of the RADC are close to the experimental ones if the coordination numbers of the Ge, As, and S are assumed to be 4, 3, and 2, respectively. These data have made it possible to conclude that the interatomic bonds are predominantly covalent in character, but the small difference between the scattering amplitudes of the components do not make it possible to test various models of short-range order structures.

Figure 13, taken from[95], shows the RADC in the GeAsS glass. Its distinguishing feature is the presence of a convex part on the left branch of the first maximum. The interpretation of the RADC has shown that a good model of the short-range structure of the glass

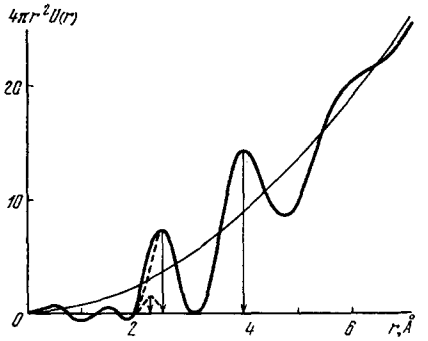

FIG. 13. Plot of the radial distribution of the atoms in the glass GeAsS.

is the model of the microheterogeneous structure, the elements of which are grouping of atoms with structure of noncrystalline compounds of germanium with sulfur and arsenic; it is not necessary here to assume the presence of groupings of atoms with As_2S_3 structure. The glass GeAsSe has apparently also a microheterogeneous structure.[95]

When the glasses GeAsS and GeAsSe are heated to 670 and 630 °C respectively, their short-range order is appreciably altered.

5) *Chalcogenides of arsenic.* Figure 14 shows RADC, taken from[96], for the crystalline, vitreous, and molten AsSI. The radial curve for the glass exhibits a significant similarity to the RADC of the crystal, but differs strongly from the RADC of the melt. The crystal structure consists of atomic chains,[97] in which As atom is covalently bound with two sulfur atoms and one iodine atom, and each S atom is bound with two arsenic atoms. The transition from the crystal to the glass does not seem to change the structure elements of the crystal significantly, but disturbs the regularity of their packing. This causes the maxima of the RADC in the glass to become more smeared out. In contrast, in crystal–melt and glass–melt transitions, changes take place in the structural elements themselves, since the value of r_1 is decreased thereby.

The change of the short-range order in the glass–melt transition for AsSeI is similar.[98]

C. Amorphous semiconductor films

1) *Elemental semiconductors.* The main structural elements of the five known crystalline modifications of boron are icosahedra,[98] which are interconnected either directly or via intermediate atoms. The interatomic bonds are of the multicenter type with electron deficiency. The structure of the short-range order of the amorphous films obtained by electron-beam evaporation of the crystal was investigated in[99]; the values obtained on the RADC are $r_1 = 1.75$ Å, $Z_1 = 5.6$, $r_2 = 3.0$ Å, $Z_2 = 17$. A comparison of the RADC in the film in different modifications of the crystal has shown that its structure is less similar to the α modification, which is stable up to 1200 °C, than to the β and τ modifications, which exist at high temperatures.

The structural variety of the condensed systems of carbon is due to the possibility of the sp^3, sp^2, and sp hybridization of the valence electrons. In the case of sp^3 hybridization, tetrahedrally directed σ bonds are produced and lead to a diamond structure. Its structural elements are tetrahedra with $r_{1a} = 1.54$ Å, $r_{2a} = 2.55$ Å and $Z_{1a} = 4$. In the case of sp^2 hybridization of the valence electrons, layered structures are produced with hexagonal arrangement of the atoms in the layers. If the period along the c axis is equal to 2, then a graphite lattice with $r_{1r} = 1.41$ Å, $r_{2r} = 2.45$ Å and $Z_{1r} = 3$ is produced. The sp hybridization leads to chain-like polymers of carbon—α and β carbyne.

The short-range structure of amorphous films can be divided into two groups. We include in the first group the data of[100,101], in which the positions of the first and second maxima of the RADC in the film, $r_1 = 1.50$ Å, $r_2 = 2.54$ Å, were found to be located between r_{1a}, r_{1r} and r_{2a}, r_{2r} respectively. This was interpreted as evidence of the coexistence of "graphite-like" and "diamond-like" groupings of atoms in the film. If it is assumed that they go over continuously into one another, then we have the classical model of a disordered grid.

The second group constitutes the results of the studies of Palatnik.[103–105] According to these data, the amorphous films of carbon are granulated objects with $R_0 \approx 12$ Å, the short-range structure of which is similar to the structure of graphite. A similar conclusion concerning the structure of amorphous films of carbon was drawn in[106].

Investigations of short-range order of amorphous films of chalcogens were considered in detail by Tatarinova.[107]

2) *Semiconductors of* III-V *type.* Under ordinary conditions, boron nitride has a hexagonal structure (α form) in which the atoms are arranged in layers in a manner similar to the arrangement in the graphite lattice. At pressures above 62 kbar and temperatures above 1300 °C, the α form goes over (in the presence of catalysts) into a cubic diamond-like modification (β form) with $a = 3.615$ Å.

Figure 15 shows the RADC in amorphous BN films, taken from[108], which yielded $r_1 = 1.73$ Å, $r_2 = 2.84$ Å, $Z_1 \approx 4$, $Z_2 \approx 11$. These data indicate a tetrahedral coordination of the nearest neighbors, as in the β form of the crystal, but the shortest interatomic distance in the

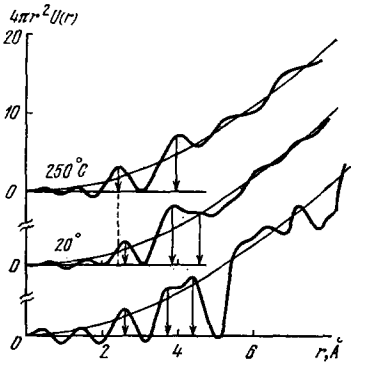

FIG. 14. Radial atomic distribution curves for crystalline (lower curve), vitreous (20 °C), and molten (250 °C) AsSI.

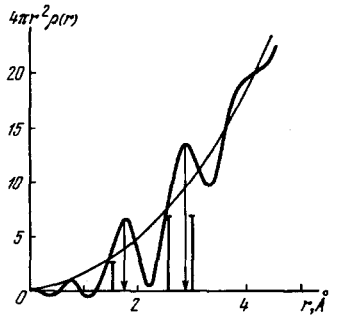

FIG. 15. Radial atom distribution curve in an amorphous BN film.

amorphous film is increased by ~11%. For amorphous films of other III-V compounds (GaAs[109], GaP[109], InSb[110], InAs[111]), a tetrahedral coordination of the nearest neighbors is also characteristic.

3) *Type* III-IV *semiconductors.* The short-range order structure of amorphous films of GaSe[112], GaTe[112] and InSe[113] is similar in form with the structure of the crystals. In InTe[114] films, a tetrahedral coordination of the nearest neighbors is realized, just as in the structural crystal-lattice elements in which the interatomic bonds between the atoms are the strongest.

4) *Type* IV-VI *semiconductors.* The short-range order structure of amorphous GeSe and GeTe films were investigated in[115-117]. The values observed for GeSe were $r_1 = 2.6$ Å and $Z_1 = 5.8$. In the opinion of the authors of[116], this is evidence of a distorted octahedral arrangement of the nearest neighbors in the films, just as in the crystal. The known data on the short-range order structure of atomic GeTe films are contradictory. In[116] they obtained $r_1 = 2.75$ Å, $r_2 = 4.05$ Å, $Z_1 = 6$, but according to the data of[117] $r_1 = 2.65$ Å, $Z_1 = 4$. The authors of[118] have shown that the short-range order of amorphous GeTe films is determined essentially by the conditions under which the films were obtained, by comparing the RADC in films obtained by thermal and laser sputtering. The values of r_1 and Z_1 for amorphous GeTe films (laser sputtering of the samples) and GeSe (thermal sputtering) were found in[118] to be close to the corresponding values for the melt.

5) *Semiconductors of the type* $A_2^VB_3^{VI}$. The crystals of antimony triselenide and trisulfide are isostructural. Figure 16 shows RADC for amorphous Sb_2S_3 and Sb_2Se_3 films; it is seen that the fluctuations of the radial density of the atoms in these films are of the same type.[119] This points to a similarity of the short-range order

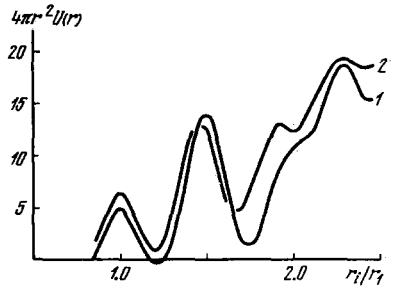

FIG. 16. Comparison of the RADC of amorphous films of Sb_2S_3 (1) and Sb_2Se_3 (2).

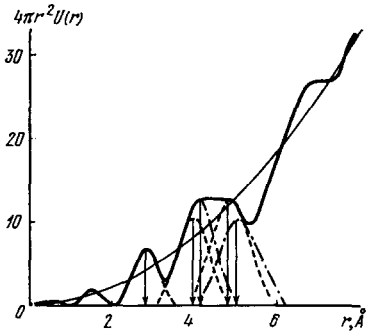

FIG. 17. Radial atom distribution in amorphous $CdGeAs_2$ film.

structure. The coordination-sphere radii and the coordination numbers for Sb_2Se_3 in the amorphous state were found to be close to the corresponding values for the melt.

The structure of the short-range order of amorphous films of arsenic chalcogenides were investigated in[120-123]. The As_2S_3 films were obtained by laser sputtering of the samples, and the RADC yielded for them the values $r_1 = 2.25$ Å, $Z_{1\,S}(As) = 3.1$, $Z_{1\,As}(S) = 2.1$, which are practically close to the corresponding values of the crystal. Coordination numbers close to those obtained are typical also of films obtained by thermal sputtering of the samples, but the shorter interatomic distance can be increased to $r_1 = 2.36$ Å.[124]

The short-range order structure of amorphous As_2Se_3 films also depends strongly on the production conditions.[121] Thus, in the case of thermal sputtering of the samples a film is condensed with an RADC that yields $r_1 = 2.25$ Å and $Z_1 = 2.2$, whereas the results obtained by laser sputtering were $r_1 = 2.0$ Å and $Z_1 = 1.8$. In both cases, the film structure is made up of atomic chains, just as in the crystal structure, with a decreased shortest interatomic distance.

The short-range order structure of amorphous As_2Te_3 films is made up of trigonal pyramids[127] of the structure elements of the crystal lattice, between the atoms of which are realized the strongest interatomic bonds.

6) *Semiconductors of type* $A^{II}B^{IV}C_2^V$. The compounds $A^{II}B^{IV}C_2^V$ have under ordinary conditions a metallic chalcopyrite lattice, which differs from the sphalerite structure in the ordered arrangement of the atoms in the cation sublattice. The short-range order structure of amorphous films of this compound was investigated in[125]. Figure 17 shows the RADC in an amorphous $CdGeAs_2$ film, from which we get $r_1 = 2.80$ Å, which exceeds by $\Delta r = 0.27$ Å the average distance to the nearest neighbors in the crystal. Different methods of resolving the second maximum of the RADC yielded the same result—the distances to the second and third neighbors in the film and crystal were close. The author of[125] has concluded that the structural units of $CdGeAs_2$ in amorphous and crystalline states are tetrahedra, and the larger value of r_1 in the film was attributed to the (statistical) displacement of the atoms from their positions in the centers of the tetrahedra in one of the vertices.

Figure 18 shows the RADC in an amorphous $CdSnAs_2$ film. Its structure elements are also tetrahedra, the

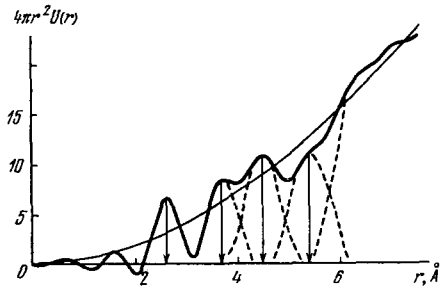

FIG. 18. Radial atom distribution in amorphous $CdSnAs_2$ film.

average distance to the nearest neighbors in which is practically equal to the corresponding value for the crystal. However, the positions of the succeeding maxima of the RADC in the film differs substantially from the average distances to the more distant neighbors in the crystal. This is due to the difference between the methods of packing of the tetrahedra in the amorphous and the crystalline states.

4. MAIN FEATURES OF THE GENERAL LAWS OF STRUCTURE FORMATION OF NONCRYSTALLINE SEMICONDUCTORS

A. Role of initial crystal structure in the formation of the short-range structure of a melt

In Table I are summarized the results of x-ray diffraction studies of the short-range structure of molten semiconductors. It indicates the types of crystal structure, the shortest interatomic distances r_1 for them, and the values of the coordination numbers $Z_{1i}(j)$.

The column marked "T, °C of the investigated melt" lists the temperatures at which the melts were investigated, followed by the position $r_{1\rho}$ of the first maximum of the RADC and the value of $Z_{1\rho}i(j)$ for the melt. If the melt structure has been investigated in a certain temperature interval, then the minimum and maximum temperatures are indicated together with the corresponding changes of $r_{1\rho}$ and $Z_{1\rho}$. Comparison of the data on the crystal structure and the short-range order of the melts can assess the role played by the initial structure of the crystal in the formation of the structure of the short-range order of the melt. This question has two aspects, connected with the similarity or difference of the structure elements of the crystal and the melt near T_m and the manners in which they are packed. Taking into account the positive or negative answers to these questions for the actual substances marked "+" and "−" in Table I, the general law governing the influence of the crystal structure on the formation of the short-range structure of the melt can be formulated as follows:

The melting of semiconductors that have homodesmic structures in the crystalline state is accompanied by a change of the short-range order, while melting substances with heterodesmic structure preserve the structure elements of the crystal.

Indeed, IV and III-V semiconductors, which have crystal lattices of the diamond and ZnS type, have in the molten state higher values of r_1 and Z_1; the short-range order structure of these melts differs greatly from the

TABLE I.

Semiconductor	Type of crystal structure	Substance	T_m, °C	Crystal			T, °C of the investigated melt	Melt			Reference	$\Delta r = r_{1\rho} - r_1$, Å	$\Delta Z' = Z_{1\rho}(j) - Z_{1i}(j)$	$\Delta Z'' = Z_{1\rho}(i) - Z_{1j}(i)$	Preservation of the structural elements of the crystal in the melt	Similarity of the packing of the atoms in the crystal and the melt
				r_1, Å	$Z_{1i}(j)$	$Z_{1j}(i)$		$r_{1\rho}$, Å	$Z_{1\rho}(j)$	$Z_{1\rho}(i)$						
A^{IV}	Diamond	Ge	937	2.44	4		940	2.75	5.7		34	0.31	1.7		−	−
							1000–1300	2.7–2.8	8–5.9		29	0.26–0.36	4–1.9		−	−
		Si	1414	2.35	4		1500	2.7	6.9		34	0.35	2.9		−	−
A^{VI}	Rhombic	S	112.8	2.059	2		130–250	2.4–2.08	2.4–2.6		46	0.14–0.02	0.4–0.6		+	−
	Hexagonal	Se	220	2.37	2		230–430	2.35–2.41	2.7–2.5		52	−0.02	0.7–0.5		+	−
												(+0.04)				
		Te	452	2.83	2		450	2.95	2.4		54	0.12	0.4		+	−
							575–1800	2.97–3.07	3–6		55	0.14–0.24	1–4		−	−
$A^{III}–B^{V}$	ZnS	GaSb	712	2.65	4	4	750–1100	3.0–3.1	5.8–6.6		57	0.35–0.45	1.8–2.6		−	−
		InSb	536	2.81	4	4	540	3.15	5.8		59	0.34	1.8		−	−
							550–725	3.4	7.7–7.3		58	0.59	3.7–3.3		−	−
		InAs	942	2.62	4	4	1000	3.18	7.6		60	0.56	3.6		−	−
$A^{III}B^{VI}$	Tl_2Se	InTe	696	2.84	4		750	3.2	6.3		62	0.36	2.3		−	−
$A_2^{III}B^{VI}$	Tetragonal	Tl_2Se	390				460				64				+	+
$A_2^{III}–B_3^{VI}$	ZnS_{def}	In_2Te_3	667	2.67	2.66	4	700	2.90	2.5	3.75	64	0.23	−0.16	−0.2	+	
$A^{IV}–B^{VI}$	Rhombohedral	GeSe	670	2.96	6	6	670	2.50	4	4	66	−0.46	−2.0	−2.0	+	−
		GeTe	724	3.01	6	6	730	2.70	(2)	4	66	−0.31	(−4.0)	−2.0	+	−
	NaCl															
$A_2^{V}–B_3^{VI}$	Monoclinic	As_2S_3	310	2.25	2	3	420	2.30	2.5	3.8	69	0.05	0.5	0.8	+	−
		As_2Se_3	360	2.36	2	3	450	2.45	2.35	3.5		0.09	0.35	0.5	+	−
	Rhombic	Sb_2Se_3	605	2.66	3	5	620	2.75	3.2	4.8	70	0.09	0.2	−0.2	+	−
	Rhombohedral	Sb_2Te_3	622	3.21	6	6	640–680	3.16–3.10	5.4–4.7		70	−(0.05–0.1)	−(0.6–1.3)		+	+
$A^{V}–B_3^{VII}$	PbI_2	AsI_3	140	2.58	2	6	145	2.65	1.07	3.2	71	0.07	−0.93	−2.8	+	−
		SbI_3	171	2.75	2	6	175	2.75	1.2	3.4	71	0	−0.80	−2.6	+	−

structure of the crystal. Somewhat lower values of the coordination numbers in the liquid Ge and InSb near T_m when in the case of high temperatures seem to indicate a "looser" packing of the atoms, which becomes denser when the melts are heated. This, however, is the only thing left in them "from the crystal."

The elements and compounds with strong (covalent or ion-covalent) and weak (van der Waals) bonds in their crystal lattice, are, as it were, prepared for the formation of melts consisting of the same structure elements as the crystal. The packing of the neighbors which is inherent in the crystal is preserved in this case only for such substances (Sb_2Te_3, Te_2Se), in which entire packets, consisting of a large number of layers, go over into the melt upon melting. It is interesting, that besides the structure elements of the crystal phase, which are thermodynamically stable near T_m, there can be produced in the melt also structure elements of metastable (Se) low-temperature modifications of the crystals (GeTe). Their coexistence is apparently due to the dynamic properties of the liquid and primarily to the fluctuation instability of its structure, which gives rise to the "virtual" character of the molecular complexes.[126]

The compounds $A_2^{III}B_3^{VI}$ are isoelectronic analogs of the III-V compounds, which melt with an appreciable change of the short-range order. They also have a ZnS crystal lattice, but with defects, in which 1/3 of all the cation-sublattice sites are vacant. There are covalent sp^3 bonds between the III and VI atoms, and from each VI atom surrounding the vacancy there is directed towards the latter an unshared pair of electrons. Orbitals with an unshared pair are not bindings, therefore the properties of the VI atoms that border on the vacancies and are located in the surroundings of the III atoms differ greatly.[63] Consequently, from the formal point of view, $A_2^{III}B_3^{VI}$ crystals can best be regarded as having a heterodesmic structure with differing III–VI bonds and with B^{VI}-vacancy "bonds." When the crystal goes over into the melt, the latter break, as a result of which the short-range structure of the melt, in contrast to III-V melts, preserves a certain similarity with the structure of the crystal (In_2Te_3).

Indium monotelluride has a heterodesmic structure, but in the melt, at a temperature ~ 50 °C above T_m, the only similarity with the crystal structure is the near equality of r_{1D} and r_1. It appears that at lower degrees of overheat of the melt this similarity will be more strongly pronounced.

B. Classification of melts

It was noted earlier that an investigation of the regularities governing the variation of the physical properties in the course of melting have enabled A. R. Regal' to classify all of the semiconductors into those melting into semiconductors and those melting into metals.[7] Later investigations have only refined this classification. In particular, Mott has shown,[127] making use of Anderson's criterion,[128] that the formation or the collapse of the pseudogap in the energy spectrum of noncrystalline substances takes place at $\sigma = 350\ \Omega^{-1}\,cm^{-1}$ (for $Z_1 = 6$), and supplemented the Regel' classification by subdividing the melts into metals, semimetals, semiconductors with a narrow forbidden gap, and tunnel semiconductors.

We have attempted to classify liquid semiconductors in accordance with a structural attribute. This classification is based on a subdivision of the melts into groups with similar coordination of the nearest neighbors near T_m. Table II indicates, besides the latter, the coordination of the neighbors in the crystals, the quantitative changes, in the course of melting, of the shortest interatomic distances $\Delta r_1(\%)$ and coordination numbers $\Delta Z_1(\%)$ (average values are used for heterodesmic structures), and the published data on the conductivity in the liquid phase near T_m, predominantly from[127]. As follows from Table II, all the melts can be broken up into five groups. The most numerous first group is made up of the semiconductors A^{IV}, $A^{III}B^{V}$, $A^{III}B^{VI}$ and Sb_2Te_3, to which an octahedral coordination of the nearest neighbors corresponds in the liquid state. Substances with geodesmic structures in the crystal state alter significantly the structure of the short-range order upon melting, and their values of Δr_1 and ΔZ_1 are large; the changes of these quantities are smaller for the semimetal (after Mott[127]) Sb_2Te_3. We note that the conductivity σ for all the melts of the first group has values that are typical of metals. Chalcogenides form the second group; when they melt, the structural elements of the crystals are predominantly preserved, and the ability to preserve the latter decreases with increasing atomic number. Δr_1 has a tendency to increase in this case, while ΔZ_1 is approximately the same for all the melts.

The third group includes chalcogenides of arsenic and tallium, which preserve the structural units of the crystals in the molten state. It appears that as a result one should expect small changes in the energy spectrum upon melting.

The fourth and fifth groups are made up of melts with predominantly tetrahedral and pyramidal coordinations of the nearest neighbors, respectively. When the crystal melts, the structure elements are preserved to a certain degree, but their packing is significantly altered. An exception is In_2Te_3, the melting of which leads to a "smearing" of the short-range order of the crystal. The values of Δr_1 and ΔZ_1 for these substances are large and frequently negative. The latter undoubtedly is evidence that the covalent component of the interatomic bonds increases on melting.

A rise in temperature can lead to significant changes in the coordination of the nearest neighbors in the melt. Thus, when the melt of Te is heated to 1700 °C, Z_1 increases to ~ 6. At this temperature, the melt must be regarded as belonging to the first group. We will recall therefore that the arrangement of the substances in Table II corresponds to their structural features near T_m.

We note that Table II implies an interesting common regularity in the variation of the short-range order of melting semiconductors: *melts of isostructural crystals have similar short-range structures* that contain similar structure elements. By way of example, we can

TABLE II. Classification of semiconductor melts.

Coordination of the nearest neighbors in the melt	Coordination of the nearest neighbors in the crystal	Substance	$\Delta r = \frac{r_{1p} - r_1}{r_1}$, %	$\Delta Z = (Z_{1p} - Z_1)/Z_1$, %		σ, Ω^{-1} cm^{-1}, of the melt
				$i(j)$	$j(i)$	
Octahedral	Tetrahedral	Ge	10–14	42–100		14000
	Tetrahedral	Si	14	72		12000
	Tetrahedral	GaSb	13.2	45	45	10600
	Tetrahedral	InSb	12–21	45–92		10000
	Tetrahedral	InAs	21.4	90	90	6800
	Tetrahedral + octahedral	InTe	13	33		1500
	Distorted NaCl	Sb_2Te_3	1.6	10		1800
Chains and rings	Rings	S	0.5–0.9	11–20		10^{-12}
	Chains	Se	−0.8–2.5	25–35		10^{-9}
	Chains	Te	2.4–4.2	15–20		1755
Layered	Layered	As_2S_3	2.2	25	27	10^{-10}
		As_2Se_3	3.8	17	16	10^{-5}
	Layered + molecular	Tl_2Se				3
Tetrahedral	Distorted NaCl	GeSe	−15.5	−33	−33	50
	Tetrahedral	In_2Te_3	8.6	−6.1	−6.2	79
Pyramidal	Ribbons	Sb_2Se_3	3.4	6.7	−4	2
	Layered	AsI_3	2.7	−46	−47	
	Layered	SbI_3	0	−40	−43	

point to the semiconductors A^{IV}, $A^{III}B^{V}$, $A_2^{V}B_3^{VI}$, $A^{V}B_3^{VII}$.

The converse, however, is not true: *melts with similar structure of the short-range order do not correspond to isostructural crystals*. By way of examples of this situation we can point to substances constituting the first group of the presented classification.

C. Change of short-range order in a transition of the semiconductor–metal type

It follows from Table II that melts of the first group are characterized by large values of the conductivity, greatly exceeding $\sigma = 350\ \Omega^{-1}\,cm^{-1}$—the boundary between semiconductors and metals. Taking into account the variety of the structural types of crystals of these substances and the structural similarity of the melts, we can conclude that *the semiconductor–metal transition is from a structural point of view a transition from a crystal structure to a melt short-range structure characterized by a predominantly octahedral coordination of the nearest neighbors*. The transition can take place at the melting temperature (Sb_2Te_3), at a slight overheating of the melt (A^{IV}, $A^{III}B^{V}$), or at a considerable overheating (Te). The changes of Δr_1 and ΔZ_1 are in this case 10–21% and 33–100%, respectively.

D. Short-range order changes in a transition of the semiconductor–semiconductor type

The substances listed in Table II and having in the molten state $\sigma < 350\ \Omega^{-1}\,cm^{-1}$ melt in accordance with the semiconductor–semiconductor scheme. These substances, with respect to the character of the change of the short-range order, can be divided into two groups.

The first group includes the semiconductors A^{VI}, $A_2^{III}B_3^{VI}$, $A_2^{III}B^{IV}$ and $A_2^{V}B_3^{VI}$, which practically preserve the nearest-neighbor coordination of the crystals when they melt. The second group includes the compounds $A^{IV}B^{VI}$ and $A^{V}B_3^{VII}$, whose transition into the liquid state leads to a significant change of the crystal coordination of the atoms, while the structural elements of the crystals are preserved to a certain degree.

When semiconductors of the first group melt, the shortest interatomic distances have a tendency to increase, and the resultant looser packing of the nearest neighbors can be compensated for (in part) by a small increase of the coordination numbers ($\Delta Z_1 = 7$–35%). Melting of the semiconductors of the second group leads

TABLE III.

Substance	State	T, °C	Position of the maximum RADC, A					R_0, Å	A_1 exp	$Z_{1i}(j)$	$Z_{1j}(i)$	l_{exp}	Reference
			r_1	r_2	r_3	r_4	r_5						
Se	Melt	430	2.41	3.75	5.2			7.6	2.5	2.4		0.55	52
		230	2.38	3.75	4.8	5.9		7.5	2.7	2.5		0.54	
	Glass	20	2.40	3.75	4.8	5.8		9	2.1	2.06		0.50	
As_2S_3	Melt	420	2.30	3.50	4.3	5.4	6.4	9	2.6	3.8	2,5	0.54	68
	Glass	20	2.30	3.50	4.2	4.9	5.8	10	2.9	4.2	2,8	0.58	84
As_2Se_3	Melt	450	2.45	3.65	4.3	5.2	6.1	8.4	2.8	3.5	2,3	0.48	89
	Glass	20	2.42	3.7	4.6	5.6	6.4	9.5	2.8	3.5	2,3	0.58	
AsSe	Melt	510	2.46	3,7	4.3	5.8	7.2	8	3.3	3.2	3,2	0.54	89
	Glass	20	2.45	3.8		5.8	7.0	10	3.4	2.9	2,9	0.48	
Ge_2S_3	Melt	400	2.3	3.75				9	2.7			0.90	
	Glass	20	2.26	3.65	4.35	5.1	5.7	9	2.8			0.43	
Ge_9Se_{91}	Melt	450	2.35	3.8	5.2	6.0		8	3.0			0.53	
	Glass	20	2.35	3.8	4.8	5.8		8	3.0			0.54	94
AsSJ	Melt	250	2.4	3.9	5.4	7.0		7,2	2.3			0.62	96
	Glass	20	2.53	3.8	4.6	5.5	6.2	7,2	1.9			0.59	
GeAsS	Melt	670	2.4	3.5	4.3			6	2.9			0.88	
	Glass	20	2,43	3.8				8.5	3.7			0.52	95
GeAsSe	Melt	630	2.5	3.7	4.3			9	3.0			0.60	
	Glass	20	2.42	3.85				12	3.6			0.55	95

TABLE IV.

Substance	State	Position of the maximum RADC, Å				$Z_{1i}(j)$	$Z_{1j}(i)$	Z_2	Z_3	Reference
		r_1	r_2	r_3	r_4					
B	Crystal	1.6–1.8	2.9–3.1			6		15		99
	Amorphous film	1.75	3.0			5.6		17		
C	Crystal	1.41	2.45	2.83	3.34	3		6	3	99
	Amorphous film	1.44	2.48		3.3	3		9		
BN	β-crystal	1.57	2.56	3.0		4		12		108
	Amorphous film	1.73	2.84			3.6		11		
GaAs	Crystal	2.44	3.96			4		12	12	109
	Amorphous film	2.44	4.04			3.4		15		
InSb	Crystal	2.82	4.6	5.4	6.7	4		12	12	58
	Melt	3.4	4.9			7.7		13.5		
	Amorphous film	3.05	4.5	5.8	6.9	4		11	13	
GaSe	Crystal	2.48	2.33	3.7		3		1	6	112
	Amorphous film	2.42		3.7		3.5			6	
InSe	Crystal	2.50	3.16			3		1		
	Amorphous film	2.75	3.8			2.9		5.3	5.6	
InTe	Crystal	2.78	3.53			4		8		
	Melt	3.2				6.2				62
	Amorphous film	2.85	4.0			3.4				114
GeSe	Crystal	2.96				6		10		
	Melt	2.50	3.75			4		12.3		66
	Amorphous film	2.50	3.85	5.1	6.0	4.8				118
GeTe	Crystal	3.01				6				
	Melt	2.7	4.0	4.3						66
	Amorphous film	2.6	4.1	5.0		3.5				118
Sb_2Se_3	Crystal	2.5–3.2				5.7	3			
	Melt	2.75				4.8	3.2			70
	Amorphous film	2.7				4.6	3.07			
As_2S_3	Crystal	2.25	3.5			3	2			
	Melt	2.3	3.5			3.8	2.5			69
	Amorphous film	2.3				3.1	2.07			
As_2Te_3	Crystal	2.7–2.8				3				
	Amorphous film	2.7	3.7			3.3	2.2			123
$CdGeAs_2$	Crystal	2.52	4.12	4.84		4				125
	Amorphous film	2.80	3.9–4.1	4.9		4				
$CdSnAs_2$	Crystal	2.62				4				125
	Amorphous film	2.65				3.5				

to a strong decrease of the coordination numbers ($\Delta Z_1 = -(4–47)\%$); the shortest interatomic distances also decrease in this case or else remain practically unchanged.

E. Measurements of the short-range order in the melt–glass transition

In Table III are compiled the known data on the short-range structure of chalcogenide semiconductors in the melt near T_m and in the glasslike state. Besides the positions r_i of the RADC maxima, the table lists the radii R_0 of the ordered arrangement of the atoms, calculated from[129], the experimental values of the areas $A_{1\,exp}$ under the first maximum of the RADC, the values of the coordination numbers $Z_{i(j)}$, and the calculated values of the integral width of the first maximum $L_{exp} = A_{1\,exp}/H_{1\,exp}$ ($H_{1\,exp}$ is the height of the first RADC maximum at $r = r_1$). Analysis of the data of Table III leads to the following conclusions:

1. In accordance with the character of the short-order in the melt–glass transition, all the substances can be divided into three groups. The first includes Se, As_2S_3, As_2Se_3, Ge_2S_3 and Ge_9S_{91}, which preserve in the vitreous state a structural similarity to the melts (but not identity). This similarity is restricted to near equality of A_1 and of the positions of two or three maxima of the RADC, but at large distances the radial curves are quite different. The second group consists of AsSI, GeAsS, GeAsSe, for which the structural similarity in the vitreous and in the molten states is either nonexistent or less pronounced (AsSe).

2. In all the substances, the region of ordered arrangements of the atoms manifests a tendency to increase in the course of the melt–glass transition, the maximum increase of R_0 reaching 40%. The integral

width of the first RADC maximum, to the contrary, decreases. The latter may turn out to be incorrect for melts whose solidification results in bonds of greatly differing lengths between the nearest neighbors, which are not typical of the liquid state.

F. Measurements of the short-range order in the transition crystal–(vapor)–amorphous film

The results of the investigations of the short-range order structure of amorphous films of semiconductors, reported in Sec. C) of Chap. 3, greatly supplement the known data.[107,130] They are compared in Table IV with the structural data for crystals and melts. We shall preface the general conclusions that follow from such a comparison by the following remarks.

The structure of the amorphous films of B, C, and of III-V and III-VI compounds is made up of the same (or similar) structural elements as the known crystal modifications. To the contrary, amorphous GeSe, GeTe, and Sb_2Se_3 exhibit a greater structural similarity with the melt than with the crystal. The short-range order structure of such melts and films, as noted in Secs. A) and C) of Chap. 3, is also made up of structural elements of crystals, the packing of which ensures a different coordination of the nearest neighbors than in crystals. The compounds $A_2^{V}B_3^{VI}$ and $A^{II}B^{IV}C_2^{V}$ in the amorphous state also contain structural elements of the crystals with packing manners which are either similar or different. Consequently:

1) In the crystal–(vapor)–amorphous film transition, the most general case is preservation of the structural elements of the crystals corresponding to the shortest interatomic distances and low values of the coordination numbers.

2) The packing of the structure elements can ensure similarity of the short-range order of an amorphous film and a crystal, a difference in the distribution of the more distant neighbors, or a new coordination of the nearest neighbors not possessed by the crystal, but which is realized in the molten state. The latter shows that[3] the well known subdivision[131] of amorphous films into "crystal-like" and "liquid-like" is based not on the difference between the structural elements, as may seem at first glance, but on the substantial difference between the manner of their packing.

[1]A. I. Blum and A. R. Regel', Zh. Tekh. Fiz. 21, 316 (1951).
[2]A. I. Blum, N. P. Mokrovskiĭ, and A. R. Regel', *ibid.*, 273.
[3]N. P. Mokrovskiĭ and A. R. Regel', Zh. Tekh. Fiz. 22, 1281 (1952).
[4]B. T. Kolomiets and T. F. Nazarova, in: Fiz. Tverd. Tela (Leningrad) (Sov. Phys. Solid State), Vol. 2, Leningrad, Izd-vo Akad. Nauk SSSR, 1959, p. 22.
[5]B. J. Kolomietz, Phys. Stat. Sol. 7, 359 (1964).
[6]A. F. Ioffe, Izv. Akad. Nauk SSSR Ser. Fiz. 15, 477 (1951).
[7]A. R. Regel', Doctoral Dissertation (Leningrad, Phys. Tech. Inst. USSR Acad. Sci., 1956).
[8]A. F. Ioffe and A. B. Regel', Progr. Semicond. 4, 237 (1960); see also Izbrannye trudy (Collected Works) A. F. Ioffe, Vol. 2, Nauka, 1975.
[9]V. M. Glazov, Doctoral Dissertation (Moscow Inst. of Steel and Alloys, 1966).
[10]V. M. Glazov, S. N. Chizhevskaya, and N. N. Glagoleva, Zhidkie poluprovodniki (Liquid Semiconductors), Nauka, 1967.
[11]D. Turnbull and M. H. Cohen, J. Chem. Phys. 29, 1049 (1958).
[12]D. Turnbull and M. H. Cohen, Nature 189, 131 (1961).
[13]L. S. Palatnik, M. Ya. Fuks, and V. M. Kosevich, Mekhanizm obrazovaniya i substruktura kondensirovannykh plenok (Mechanism of Formation and Substructure of Condensed Films), Nauka, 1972.
[14]R. W. James, Optical Principles of the Diffraction of X Rays, Bell, London, 1948.
[15]C. N. J. Wagner, J. Vac. Sci. and Technol. 6, 650 (1969).
[16]A. S. Lashko, Zh. Fiz. Khim 33, 1730 (1959).
[17]Yu. G. Poltavtsev and V. N. Gurenko, Izv. Akad. Nauk SSSR Ser. Metally No. 5, 122 (1974).
[18]E. H. Henninger, R. C. Buschert, and L. R. Heaton, J. Chem. Phys. 44, 1758 (1966).
[19]J. E. Enderby, D. M. North, and P. A. Edelstaff, Phil. Mag. 14, 961 (1966).
[20]S. Steeb and R. Hezel, Zs. Metallkunde 57, 374 (1966).
[21]N. C. Halder and C. N. J. Wagner, J. Chem. Phys. 47, 4385 (1967).
[22]J. E. Enderby, D. M. North, and P. A. Edelstaff, Adv. Phys. 16, 171 (1967).
[23]H. F. Bühner, and S. Steeb, Zs. Naturforsch. 25a, 1862 (1970).
[24]C. N. J. Wagner, N. C. Halder, and D. M. North, Phys. Lett. A25, 663 (1967).
[25]C. N. J. Wagner and N. C. Halder, Adv. Phys. 16, 167 (1967).
[26]H. F. Buhner and S. Steeb, Zs. Naturforsch, 24a, 428 (1969).
[27]H. Hendus, Zs. Naturforsch. 2a, 505 (1947).
[28]V. I. Danilov, Stroenie i kristallizatsiya zhidkostei (Structure and Crystallization of Liquids), Kiev, Izd-vo Akad. Nauk Ukr. SSSR, 1955.
[29]A. S. Lashko, in: Struktura metallicheskikh splavov (Structure of Metallic Alloys), Kiev, Naukova Dumka, 1966, p. 96.
[30]H. Krebs, V. B. Lasarev, and M. Hauke, Angew, Chem. 70, 466 (1968).
[31]S. P. Isherwood, B. R. Orton, and R. Manaila, J. Non-cryst. Sol. 8–10, 691 (1972).
[32]G. I. Batalin and V. P. Kazamirov, Kristallografiya 15, 850 (1970) [Sov. Phys. Crystallogr. 15, 739 (1971)].
[33]A. S. Lashko and Yu. G. Poltavtsev, Ukr. Fiz. Zh. 12, 871 (1967).
[34]Yu. G. Poltavtsev, Kristallografiya 16, 456 (1972) [Sov. Phys. Crystallogr. 16, 387 (1972)].
[35]C. B. Walker and D. T. Keating, Acta Cryst. 14, 1170 (1961).
[36]P. L. Maitrepierre, J. Appl. Phys. 40, 4826 (1969).
[37]É. A. Pastukhov and N. A. Vatolin, in: Tezisy dokladov Vsesoyuznoi konferentsii po khimicheskoi svyazi v poluprovodnikakh i polumetallakh (Abstracts, 5th All-Union Conf. on Chemical Bond in Semiconductors and Semimetals), Minsk, AN BSSR, 1974, p. 44.
[38]O. Foss, Acta Chem. Scand. 7, 1221 (1953).
[39]B. Meyer, Chem. Rev. 64, 429 (1964).
[40]A. H. Blatchford, Proc. Phys. Soc. 45, 493 (1933).
[41]S. R. Das, Ind. J. Phys. 12, 163 (1938).
[42]S. R. Das and K. Das Gupta, Nature 143, 332 (1939).
[43]N. S. Gingrich, J. Chem. Phys. 8, 29 (1940).
[44]J. Prins, Physica 20, 124 (1954).
[45]C. W. Tompson and N. S. Gingrich, J. Chem. Phys. 31, 1598 (1959).
[46]Yu. G. Poltavtsev and Yu. V. Titenko, Zh. Fiz. Khim. 49, 301 (1975).
[47]H. Crebs, Fundamentals of Inorganic Crystal Chemistry, McGraw, 1969.
[48]H. Richter and G. Breitling, Zs. Naturforsch, 26a, 1699 (1971).

[49]H. Richter and G. Breitling, *ibid.*, S. 2074.
[50]D. R. McCann and L. Cartz, J. Chem. Phys. **56**, 2552 (1972)
[51]J. Moscinski, A. Renninger, and B. L. Averbach, Phys. Lett. **A42**, 453 (1973).
[52]Yu. G. Poltavtsev, Zh. Fiz. Khim. **49**, 307 (1975).
[53]R. Buschert, J. G. Geib, and K. Lark-Horovitz, Phys. Rev. **98**, 1157 (1955).
[54]Yu. G. Poltavtsev, Zh. Fiz. Khim. **49**, 738 (1975).
[55]G. Tourand, B. Cabane, and M. Breuil, J. Non-cryst. Sol. **8–10**, 676 (1972).
[56]N. N. Sirota and N. M. Olekhnovich, Dokl. Akad. Nauk SSSR, **136**, 660 (1961).
[57]Yu. G. Poltavtsev, Zh. Fiz. Khim. **45**, 1861 (1971).
[58]Yu. G. Poltavtsev, Fiz. Tekh. Poloprovodn. **5**, 1470 (1971) [Sov. Phys. Semicond. **5**, 1287 (1972)].
[59]J. Krebs, H. Weyand, and M. Hauke, Angew. Chem. **70**, 468 (1958).
[60]Yu. G. Poltavtsev, Zh. Fiz. Khim. **45**, 2938 (1971).
[61]V. M. Glazov and S. N. Chizhevskaya, Fiz. Tverd. Tela (Leningrad) **4**, 1841 (1962) [Sov. Phys. Solid State **4**, 1350 (1963)].
[62]Yu. G. Poltavtsev and V. M. Pozdnyakova, Zh. Fiz. Khim. **50**, 577 (1976).
[63]L. S. Palatnik, V. M. Koshkin, and Yu. F. Komnik, in: Khimicheskaya svyaz' v poluprovodnikakh i tverdykh telakh (Chemical Bond in Semiconductors and Solids), Minsk, Nauka i Tekhnika, 1965, p. 301.
[64]Yu. G. Poltavtsev, Kristallografiya **21** No. 6 (1976) [Sov. Phys. Crystallogr. **21**, No. 6 (1976)].
[65]N. Kh. Abrikosov, V. F. Bankina, L. V. Poretskaya, E. V. Skudnova, and L. E. Shelimova, Poluprovodnikovye soedineniya, ikh polychenie i svoistva (Semiconductor Compounds their Production and Properties), Nauka, 1967.
[66]Yu. G. Poltavtsev, Ukr. Fiz. Zh. **20**, 1009 (1975).
[67]M. Hansen and K. Anderko, Constitution of Binary Alloys, McGraw, 1958.
[68]Yu. G. Poltavtsev, Zh. Fiz. Khim. **49**, 1689 (1975).
[69]Yu. G. Poltavtsev, *ibid.*, p. 1692.
[70]Yu. G. Poltavtsev and S. S. Nedosekova, Kristallografiya **20**, 677 (1975) [Sov. Phys. Crystallogr. **20**, 415 (1975)].
[71]Yu. G. Poltavtsev and S. S. Nedosekova, Kristallografiya **21**, 435 (1976) [Sov. Phys. Crystallogr. **21**, 241 (1976)].
[72]H. Rawson, Inorganic Glass Forming Systems, Academic, 1967.
[73]R. Kaplow, T. A. Rowe, and B. L. Averbach, Phys. Rev. **168**, 1068 (1968).
[74]H. Richter, J. Non-cryst. Sol. **8–10**, 388 (1972).
[75]H. Krebs, Forschungsber. Landes Nordrhein–Westfallen, Nr. 1596, 3 (1967).
[76]H. Krebs, F. Schultze-Gebhardt, and R. Thees, Zs. anorg. und allg. Chem. **282**, 177 (1955).
[77]H. Hendus, Zs. Phys. **119**, 265 (1942).
[78]S. S. Flaschen, A. D. Pearson, and W. P. Northover, J. Appl. Phys. **31**, 219 (1960).
[79]A. A. Vaĭpolin and E. A. Poraĭ-Koshits, Fiz. Tverd. Tela (Leningrad) **2**, 1656 (1960) [Sov. Phys. Solid State **2**, 1500 (1961)].
[80]A. A. Vaĭpolin and E. A. Poraĭ-Koshits, Fiz. Tverd. Tela (Leningrad) **5**, 246 (1963) [Sov. Phys. Solid State **5**, 178 (1963)].
[81]J. I. Petz, R. F. Kruh, and G. C. Amstutz., J. Chem. Phys. **34**, 526 (1961).
[82]T. E. Hopkins, R. A. Pasternak, E. S. Gould, and J. R. Henderson, *ibid.*, **66**, 733 (1962).
[83]S. Tsuchihashi and Y. Kawamoto, J. Ceram. Assoc. Japan **77**, 34 (1969).
[84]Yu. G. Poltavtsev, Zh. Fiz. Khim. **49**, 1429 (1975).
[85]Yu. G. Poltavtsev and V. M. Pozdnyakova, Ukr. Fiz. Zh. **18**, 1150 (1973).
[86]V. P. Zakharov and A. P. Knyazev, Izv. Akad. Nauk SSSR Ser. Neorg. Mater. **9**, 891 (1973).
[87]Yu. G. Poltavtsev, V. M. Pozdnyakova, and V. P. Rubtsov, Ukr. Fiz. Zh. **18**, 915 (1973).
[88]A. L. Renninger and B. L. Averbach, Phys. Rev. **B8**, 1507 (1973).
[89]Yu. G. Poltavtsev, Paper at Fifth Symposium on Semiconductor Material Research, Uzhgorod, Ukr. SSR, 1974.
[90]Lyu Tsyun'-khua, A. S. Pashinkin, and A. V. Novoselova, Dokl. Akad. Nauk SSSR **151**, 1635 (1963).
[91]Y. Kawamoto and S. Tsuchihashi, J. Amer. Ceram. Soc. **52**, 626 (1961).
[92]S. C. Rouland, S. Narasimhan, and A. Bienenstock, J. Appl. Phys. **43**, 2441 (1972).
[93]H. Krebs and H. Welte, J. Sol. State. Chem. **2**, 182 (1970).
[94]Yu. G. Poltavtsev and V. M. Pozdnyakova, Zh. Fiz. Khim. **49**, 1560 (1975).
[95]Yu. G. Poltavtsev and V. M. Pozdrnyakova, Izv. Akad. Nauk SSSR Ser. Neorg. Mater. **10**, 1932 (1974).
[96]Yu. G. Poltavtsev, *ibid.*, **11**, 1742 (1975).
[97]Yu. G. Poltavtsev, V. P. Zakharov, and V. S. Gerasimenko, in: Proc. of the Conference on Amorphous Semiconductors-74, Vol. 1, Rheinhartsbrun, 1974, p. 264.
[98]G. V. Samsonov, L. Ya. Markovskii, A. F. Zhigan, and M. G. Valyashko, Bor, ego soedineniya i splavy (Boron, Its Compounds and Alloys), Kiev, Izd-vo Akad. Nauk Ykr. SSSR, 1960.
[99]Yu. G. Poltavtsev, V. P. Zakharov, and V. M. Pozdnyakova, Kristallografiya **18**, 425 (1973) [Sov. Phys. Crystallogr. **18**, 270 (1973)].
[100]H. Richter, C. Breitling, and F. Herre, Zs. angew. Chem. 8, 433 (1956).
[101]J. Kakinoki and T. Ino, Acta Cryst. **10**, 829 (1957).
[102]Y. Kamiya, J. Phys. Soc. Japan 13, 1144 (1958).
[103]B. T. Boĭko, L. S. Palatnik, A. S. Derevyanchenko, and Yu. M. Voronin, Fiz. Tverd. Tela (Leningrad) **10**, 656 (1968) [Sov. Phys. Solid State **10**, 520 (1968)].
[104]B. T. Boĭko, L. S. Palatnik, and A. S. Derevyanchenko, Dokl. Akad. Nauk SSSR **179**, 316 (1968) [Sov. Phys. Dokl. **13**, 237 (1968)].
[105]B. T. Boĭko, L. S. Palatnik, and A. S. Derevyanchenko, Fiz. Tverd. Tela (Leningrad) **13**, 611 (1971) [Sov. Phys. Solid State **13**, 499 (1971)].
[106]Yu. G. Poltavtsev, V. P. Zakharov, and V. N. Chugaev, Kristallografiya **16**, 415 (1971) [Sov. Phys. Crystallogr. **16**, 341 (1971)].
[107]L. I. Tatarinova, Élektronografiya amorfnykh veshchestv (Electron Diffraction Investigations of Amorphous Substances), Nauka, 1972.
[108]Yu. G. Poltavtsev and V. P. Zakharov, in: Tezisy dokladov II Respublikanskogo soveshchaniya) Abstracts of Paper at Second Republic Conference), Uzhgorod Univ. Press, 1975. p. 161.
[109]Yu. G. Poltavtsev, V. P. Zakharov, V. M. Pozdnyakova, and I. M. Protas, Kristallografiya **17**, 203 (1972) [Sov. Phys. Crystallogr. **17**, 165 (1972)].
[110]B. G. Poltavtsev and T. V. Remizovich, Izv. Akad. Nauk SSSR Ser. Neorg. Mater. **9**, 894 (1973).
[111]L. I. Tatarinova, Kristallografiya **15**, 853 (1970) [Sov. Phys. Crystallogr. **15**, 742 (1971)].
[112]Yu. G. Poltavtsev, V. P. Zakharov, and V. I. Shvets, Ukr. Fiz. Zh. **18**, 2049 (1973).
[113]L. I. Tatarinova and T. S. Kazmazovskaya, Kristallografiya **6**, 668 (1961) [Sov. Phys. Crystallogr. **6**, 538 (1962)].
[114]V. P. Zakharov, V. S. Gerasimenko, V. I. Zaliva, Yu. G. Poltavtsev, V. N. Chugaev, and G. P. Sheremet, Dokl. Akad. Nauk SSSR **209**, 108 (1973).
[115]F. Betts, A. Bienestock, and S. R. Ovshinsky, J. Non-cryst. Sol. **4**, 554 (1970).
[116]A. G. Mikolaĭchuk and A. N. Kogum, Kristallografiya **15**, 353 (1970) [Sov. Phys. Crystallogr. **15**, 294 (1970)].
[117]D. B. Done, M. B. Heritage, K. L. Choprd, and S. K. Bahl, Appl. Phys. Lett. **16**, 138 (1970).

[118]Yu. G. Poltavtsev and V. P. Zakharov, Kristallografiya 18, 605 (1973) [Sov. Phys. Crystallogr. 18, 379 (1973)].
[119]Yu. G. Poltavtsev and V. P. Zakharov, Kristallografiya 19, 668 (1974) [Sov. Phys. Crystallogr. 19, 416 (1974)].
[120]Yu. G. Poltavtsev, V. P. Zakharov, I. M. Protas, T. V. Remizovich, and V. N. Chugaev, Ukr. Fiz. Zh. 18, 752 (1973).
[121]Yu. G. Poltavtsev, V. P. Zakharov, V. M. Pozdnyakova, and T. V. Temizovich, Izv. Akad. Nauk SSSR Ser. Neorg. Mater. 9, 907 (1973).
[122]Yu. G. Poltavtsev, V. P. Zakharov, and I. M. Protas, in: Poluprovodnikovaya tekhnika i mikroelektronika (Semiconductor technology and microelectronics), No. 16, Kiev, Naukova Dumka, 1974, p. 62.
[123]Yu. G. Poltavtsev, V. P. Zakharov, and V. I. Shvets, Ukr. Fiz. Zh. 18, 663 (1973).
[124]P. A. Young and W. G. Thege, Thin Solid Films 7, 41 (1971).
[125]Yu. G. Poltavtsev, Izv. Akad. Nauk SSSR Ser. Neorg. Mater. No. 12 (1976).
[126]V. A. Alekseev, A. A. Andreev, and V. Ya. Prokhorenko, Usp. Fiz. Nauk 106, 393 (1972) [Sov. Phys. Usp. 15, 139 (1972)].
[127]N. F. Mott and E. A. Davis, Electronic Processes in Non-Crystalline Materials, Oxford, 1971.
[128]P. W. Anderson, Phys. Rev. 109, 1492 (1958).
[129]A. S. Lashko and Yu. G. Poltavtsev, Ukr. Fiz. Zh. 13, 1578 (1968).
[130]R. Grigorovici, J. Non-cryst. Sol. 1, 303 (1969).
[131]H. Richter and S. Steeb, Zs. Metallk. 50, 369 (1959).

Translated by J. G. Adashko

Modification of a magnetic field by plasma mechanisms

S. I. Vaĭnshteĭn

Siberian Institute of Terrestrial Magnetism, Ionosphere, and Radiowave Propagation, Siberian Division, USSR Academy of Sciences, Irkutsk
Usp. Fiz. Nauk **120**, 613–645 (December 1976)

The review is devoted to the question of the rapid modification (generation, damping, etc.) of a magnetic field in a collision-dominated plasma, when the frequency γ of the process is lower than the electron-collision frequency ν. The universally employed approach—the dynamo theory—is discussed in Chap. 2. The simplest motions that lead to generation, to rapid annihilation of the "antidynamo", and to a modification of the topological-pumping type are indicated. The discussion concerns problems of the turbulent dynamos (where a functional approach is used) and of the nonlinear dynamo. In the latter case, the Gibbs ensemble is used; a reverse cascade of magnetic and kinetic energy into the region of small wave numbers is observed. Other plasma mechanisms are discussed, namely the modification of the field by ion sound, the weakly-ionized plasma, and the solid-state plasma (dynamo based on thermal effects)—Chap. 3. It is shown that the modification can be quite effective. Discussed in Chap. 4 are high-frequency oscillations (whistlers, Langmuir oscillations) and their role in the modification of the field. The indicated mechanisms can be effective under conditions of the solar chromosphere.

PACS numbers: 52.35.Ck

CONTENTS

1. Introduction 987
2. New Topics in the "Old" Theory 988
3. Low Frequencies 998
4. High Frequencies 1002
5. Conclusion 1004
References 1004

1. INTRODUCTION

The question of modification of magnetic fields is important for many applications. Thus, after the discovery of the magnetic fields of the sun, the stars, and the interstellar gas, the question arose of the origin of these fields. Another aspect of this problem is the rapid destruction or annihilation of these fields (solar flare, the frontal point of the magnetosphere, the tail of the magnetosphere, z-pinch, etc.). As a rule, the plasma is not strongly collision-dominated here, so that the dissipation is low. The magnetic field is "frozen-in" into the medium, and the annihilation proceeds quite slowly. How are we then to explain the observed rather rapid modification of the field?

The "classical" approach to this problem is that of the dynamo theory, in which the entire responsibility for the modification is placed on the hydrodynamic motions. The latest review of this problem was published in our country in 1972.[1]

Abroad, reviews were published by Stix,[2] Gubbins,[3] Soward and Roberts,[4] and Rädler.[5] Since that time, major, principally qualitative, changes took place in the theory. In recent years, a tendency to "come down to earth" has been noted. On the one hand, papers were published using a simple velocity field that lends itself to laboratory simulation,[6–13] and on the other hand there are works that do not confine themselves to the magnetohydrodynamics approximation and use a larger